

See discussions, stats, and author profiles for this publication at: <https://www.researchgate.net/publication/231632386>

Binding behavior of crystalline and noncrystalline phases: evaluation of the enthalpic and entropic contributions to the separation selectivity of nonpolar solutes with a novel chr...

ARTICLE *in* THE JOURNAL OF PHYSICAL CHEMISTRY B · OCTOBER 2002

Impact Factor: 3.3 · DOI: 10.1021/jp0200371

CITATIONS

24

READS

15

4 AUTHORS, INCLUDING:



Reinhard Ingemar Boysen

Monash University (Australia)

102 PUBLICATIONS 947 CITATIONS

SEE PROFILE



Hirotaka Ihara

Kumamoto University

313 PUBLICATIONS 3,940 CITATIONS

SEE PROFILE

Binding Behavior of Crystalline and Noncrystalline Phases: Evaluation of the Enthalpic and Entropic Contributions to the Separation Selectivity of Nonpolar Solutes with a Novel Chromatographic Sorbent

M. A. Jamil Chowdhury,[†] Reinhard I. Boysen,[†] Hirotaka Ihara,[‡] and Milton T. W. Hearn^{*,†}

Australian Centre for Research on Separation Science, Centre of Bioprocess Technology, Department of Biochemistry and Molecular Biology, Monash University, Clayton, Victoria, Australia 3168, and Graduate School of Science and Technology, College of Engineering, Kumamoto University, 2-39-1 Kurokami, Kumamoto 860-8555, Japan

Received: January 9, 2002; In Final Form: June 4, 2002

In this paper, we describe studies of the retention characteristics of nonpolar molecules with a novel liquid-crystalline, silica-supported, comb-shaped polymer chromatographic phase, Sil-ODA₁₈. These results extend and amplify previous reports of the roles of enthalpic- and entropic-driven processes in the modulation of the selectivity of nonpolar and polar compounds in reversed-phase high-performance liquid chromatography (RP-HPLC). The investigations reveal that phase reorganization is the most important factor controlling selectivity enhancement with silica-supported, comb-shaped polymer phases as the temperature, T , of the system is varied. Moreover, these studies demonstrate that contributions from the stationary and the mobile phases can be independently fine-tuned to achieve enhanced selectivity via partition and/or adsorption binding processes. The relevant thermodynamic parameters, namely, the changes in enthalpy, entropy, and heat capacity for various nonpolar solutes with this comb-shaped polymeric sorbent, have also been determined using recently developed analytical procedures for the evaluation of nonlinear van't Hoff plots. These investigations into the thermodynamic properties of the comb-shaped polymeric sorbent in its ordered crystalline and noncrystalline states clearly delineate the differences in binding behavior compared to conventional types of monolayer n -alkylsilica sorbents and thus should facilitate wider application of this new class of reversed-phase sorbents in the separation sciences.

Introduction

Reversed-phase chromatography (RPC) is currently the most widely used of all of the high-performance liquid chromatographic (HPLC) modes of separations. The evaluation of the physicochemical basis of the retention mechanisms of different classes of solutes in RPC has received extensive attention, with the experimental results often interpreted in terms of the solvophobic model proposed by Horvath et al.^{1,2} A central question pertaining to all RPC separations is, What drives the retention process? This question has been the subject of considerable debate and investigation since the concept of RPC was first used in 1950 as an analytical separation method by Howard and Martin.³

Two primary RPC mechanisms can be considered, namely, the solvation/desolvation model,^{1,2} whereby expulsion of solutes from a polar mobile phase dominates the free energy of transfer with nonpolar sorbents acting as receptive but passive surfaces, and the partitioning model,^{4–6} where the stationary phase contributes in a much more significant way to the overall distribution process. On the basis of solvophobic considerations that encompass the solvation/desolvation model, Horvath and co-workers¹ have proposed that the interaction between the solute and the mobile phase provides the primary driving force. According to this model, retention in the high-performance modes of RPC can then be attributed to adsorption rather than partitioning processes between the solutes and the nonpolar sorbent.^{1,2} In the solvation/desolvation model, the contribution

of the stationary phase per se is thus minimized with the retention of a solute largely controlled by the free energy liberated by the formation of water–water contacts upon binding of the solute to the passive nonpolar surface of the sorbent. Retention via solvophobic processes can then be described in terms of a two-step mechanism, which involves the creation of a solute-sized cavity in the mobile phase and the transfer of solutes to or from this cavity.

An alternative three-step partition model of retention has been proposed by Dill et al.^{4,5} on the basis of the application of mean-field statistical thermodynamic theory. This three-step process involves (i) creation of a solute-sized cavity in the stationary phase, (ii) transfer of solute from the mobile- to the stationary-phase cavity, and (iii) closing of the solute-sized cavity in the mobile phase. In the partitioning model, solutes can become fully embedded in the stationary phase rather than just adsorbed onto the surface of the sorbent. When a partition mechanism applies, solute retention will be affected by the surface density of the immobilized phase, whereas if adsorption occurs, this dependence should not apply. The fundamental differences between the partitioning model and the solvation/desolvation/adsorption model thus relate to changes in the degrees of freedom of the various components of the system associated with the binding process.

Vailaya and Horvath⁷ have examined in terms of solvophobic concepts a large body of data involving RPC separations, oil–water partitioning, and adsorption to activated charcoal of low-molecular-weight compounds from dilute aqueous solutions. The free-energy changes per unit surface area for each of these processes were found to agree with solvophobic predictions. Importantly, the results confirmed the dominant role of the

* To whom correspondence should be sent. E-mail: milton.hearn@med.monash.edu.au.

[†] Monash University

[‡] Kumamoto University.

mobile phase in governing the selectivity in RPC of nonpolar solutes. Cole and Dorsey⁸ have also calculated enthalpy and entropy changes for a number of solutes on binding to immobilized *n*-octadecyl-(C₁₈)-sorbents of low bonded densities and have compared the values obtained by Gill and Wadso⁹ for the transfer of the same solutes from bulk organic liquids to water. This comparison revealed that the chromatographic process was not directly modeled by a bulk oil–water partition process, with the nonpolar ligands anchored onto the stationary phase acting as an interphase rather than as a bulk phase.

Further, Vailaya and Horvath¹⁰ obtained thermodynamic data with RPC sorbents of various ligand densities to validate further the physicochemical basis of these solvophobic considerations. The expected effect of ligand density in these RPC systems on retention data was not, however, always observed. However, thermodynamic studies by Cole and co-workers^{8,11} have shown a consistent effect of ligand density on retention. These investigators further concluded that arguments based on the hydrophobic driving force as predicted by solvophobic concepts lead to a reasonable explanation when hydrogen-bonded or highly aqueous mobile phases were used, but invoking this “solvophobic effect” did not provide an adequate explanation for retention processes in other situations. Moreover, the selectivity trends evident with stereoisomeric solutes have yet to be rationalized in terms of solvophobic concepts, despite their application to large sets of experimental retention data related to homologous compounds. For example, Sander and Wise have reported^{12–15} unusual selectivity behavior of isomeric polycyclic aromatic hydrocarbons (PAHs) with immobilized monomeric and polymeric C₁₈ phases of various bonded densities. The structure and morphology of the immobilized ligand at the surface of the stationary phase must thus play an important role in the selectivity of PAHs and other classes of molecule.

To evaluate in a physically consistent manner the dominant driving force in RPC, two key factors therefore need special attention, namely, the state of organization of the bonded stationary phase and the polarity of the eluent. With conventional *n*-alkylsilica sorbents, various lines of evidence suggest that the binding process of solutes with these nonpolar stationary phases shifts from a partitionlike to an adsorptionlike mechanism as the length of the nonpolar ligands that form the bonded phase becomes shorter.¹⁶ DeVido et al.¹⁷ recently reported that partition processes shift from enthalpy-driven to entropy-driven with increasing *T* with such nonpolar sorbents. However, Vailaya and Horvath^{7,10} have concluded that a clear distinction between partition and adsorption processes in RPC for nonpolar solutes is not apparent from their thermodynamic analysis.

To further probe the underlying mechanism(s) that prevail in the RPC of nonpolar solutes and to gain additional insight into the origin of these apparently contradictory observations on the retention processes that arise from variations in the bonded-phase properties, a single experimental system that exhibits all of these features is needed (i.e., adsorption, partition, and a shift from an enthalpy-driven to an entropy-driven mechanism depending on the selected mobile-phase composition or *T*). We have therefore investigated for such a model system the binding behavior of a novel comb-shaped polymer (Figure 1) based on *n*-octadecyl-acryl groups, which shows all of these desired properties when immobilized¹⁸ as a silica-based sorbent (Sil-ODA₁₈). In this report, we present a quantitative evaluation of retention data of nonpolar solutes with this Sil-ODA₁₈ sorbent as a prototypical example of the thermodynamic changes that can arise when transitions occur between the crystalline and noncrystalline liquid states of immobilized phases in RPC. In

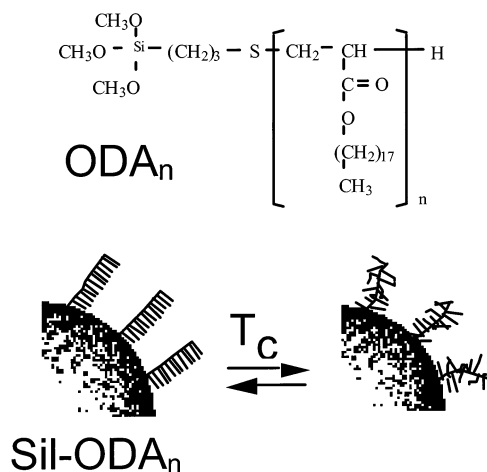


Figure 1. Schematic illustration of a silica-supported, comb-shaped polymeric sorbent (Si-ODA)_{*n*} ($8 \leq n \leq 18$) and the type of phase transition that could occur from the crystalline to the noncrystalline state as the temperature is raised.

addition, the physicochemical basis of the binding behavior of this Sil-ODA₁₈ sorbent is compared with results obtained with a more conventional type of immobilized *n*-octadecylsilica (C₁₈) sorbent.

Experimental Section

Materials. The silica-supported comb-shaped polymer sorbent (Sil-ODA₁₈) was prepared, characterized, and packed into stainless steel columns (150 × 4.6 mm) on the basis of procedures reported previously.^{18–20} A YMC silica (5 μm, 120 Å, 295 m² g^{−1}) (YMC, Wilmington, NC) was used for the immobilization of the polymer. A conventional *n*-octadecyl-modified silica sorbent (Inertsil ODS, G. L. Science, Tokyo, Japan) of similar particle (5 μm) and pore sizes (100 Å) and surface area 300 m² g^{−1} was employed for two comparative reasons. First, our previous studies had shown that similar percent carbon loadings could be achieved for both of these high-purity silicas—YMC silica and Inertsil silica—when the former was modified with Sil-ODA₁₈ groups and the latter, with *n*-octadecyldimethyl groups, despite the fact that the number of carbon atoms per mole of polymer in the case of the Sil-ODA₁₈ sorbent was 384 yet was only 20 in the case of the *n*-octadecyldimethylsilica sorbent. However, under analogous bonding conditions, comparable carbon loadings could not be achieved for the *n*-octadecyldimethyl-modified YMC silica.

Chemicals. All samples were purchased from Sigma-Aldrich (Tokyo, Japan) or Fluka Chemika-Biochemika (Tokyo, Japan), and HPLC-grade methanol was obtained from Wako Pure Chemicals (Tokyo, Japan).

Measurements. Chromatography was performed using methanol/water mixtures as the mobile phase at a flow rate of 1.0 mL min^{−1}. The chromatographic system consisted of a type 880 PU pump, a type 930 intelligent RI detector, which were both obtained from Jasco (Tokyo, Japan), a Rheodyne 7125 injection valve (Rheodyn, Cotati, CA), a type U-620 column oven (Sugai, Tokyo, Japan), and a type C-R6A data processor (Shimadzu, Tokyo, Japan). The maximum injected volume of the sample mixtures dissolved in methanol/water of different solvent percentages was 50 μL. As the sensitivity of RI detection is relatively low compared to, for example, UV detection, a larger injection volume of sample than traditionally employed with UV detection was required for accurate determinations of the *K'* values. In principle, overloading of the column as well as the RI detector can occur if excessive amounts of sample

are injected. To avoid these overloading effects, special attention was thus given in these studies to the selection of optimal experimental conditions. To achieve the highest precision in the retention data measurements, the composition of the sample solution for injection was determined by injections of mixtures of the analytes at different concentrations. The minimum concentration of an individual component in the sample mixture was determined from preliminary experiments based on achieving the highest number of theoretical plates, N , (i.e., the optimal peak shape and peak height) and the reproducibility in the retention times under the selected chromatographic conditions. This approach ensured that the data were acquired under linear isotherm conditions, with peak retention unaffected by the relatively small size of the injection volume. Moreover, the temperature of the column and mobile-phase reservoirs was controlled to be within ± 1 K. Bulk solvents were filtered and degassed by sparging with helium. The retention factor (k') measurements^{19,20} were performed under isocratic elution conditions with methanol–water mixtures at T values from 283 to 333 K in 4 K increments. The k' values were calculated in the usual manner from the relationship $k' = (t_e - t_0)/t_0$, where t_e and t_0 are the retention time of the solute and the void volume marker, respectively. The retention time of D₂O was used as the t_0 marker, with t_0 changing by less than 5% as the experimental conditions were varied over a temperature range of 50 K with the Sil-ODA₁₈ sorbent. All data points were derived from at least triplicate measurements, with t_e values between replicates varying typically by less than 1%. The various thermodynamic and extrathermodynamic parameters were calculated using the Eudoxos and Hephaestus software developed in this laboratory,^{19,20} coupled to the Excel version 5.0 program (Microsoft), whereas the statistical analysis involved the Sigmaplot 4.01 program (Jandel Scientific) linear and nonlinear regression analysis. In all figures presented, the standard deviations of replicates were smaller than the size of the data points shown. Differential scanning microcalorimetry (DSC) of the Sil-ODA₁₈ sorbent in different methanol/water combinations was carried out with a Seiko model I & E and DSC-10 apparatus (Tokyo, Japan).

Results and Discussion

Studies of the Phase Transition of the Sil-ODA₁₈ System.

When differential scanning calorimetric (DSC) measurements were carried out with the Sil-ODA₁₈ phase, the results indicated that crystalline-to-isotropic phase transitions occurred as T was varied. The first transition was observed at a temperature, T_{C1} , of ca. 303 K using 80% methanol/water (v/v) as the phase underwent a transition from the crystalline-to-liquid-crystalline state, and the second transition was observed at a temperature, T_{C2} , of ca. 313 K for the transition of the phase from the crystalline-to-isotropic state. The phase transition temperatures, T_{C1} and T_{C2} , gradually shifted to higher values with higher percentages of water in the mobile phase. Thus, the corresponding T_{C2} values at 60% (v/v) and 40% (v/v) methanol/water were ca. 315 and 317.5 K, respectively (Figure 2). In an 80% (v/v) methanol/water system, the crystalline state was detected at T values below 303 K, whereas the crystalline-to-liquid-crystalline state occurred between 303 and 313 K. Liquid crystals represent a specific state between a crystalline solid (most ordered) and an isotropic liquid (least ordered). Liquid crystals are systems that display liquidlike translational order but solidlike orientation order, with the liquid-crystalline state formed after the melting of the solid. The resulting liquid preserves properties intermediate between the solid and the liquid over a certain T range. A transition takes place at a specific T value, called the clearing temperature, to the isotropic liquid. The T difference between

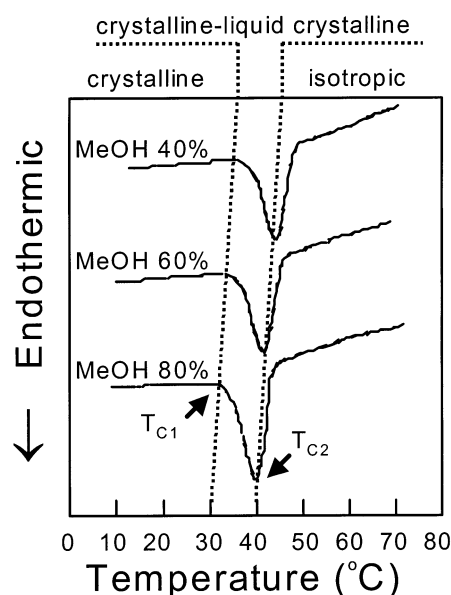


Figure 2. Differential scanning microcalorimetric thermograms of the Sil-ODA₁₈ sorbent as a methanol–water dispersion at 40, 60, and 80% (v/v) methanol (MeOH) in water, illustrating the shift in the phase-transition temperature to higher values with increasing percentages of water.

the melting point of the solid and the isotropic liquid determines the mesophase range (i.e., for the Sil-ODA₁₈ phase, this was between 303 and 313 K). As apparent from the DSC experiments, the ratio of the liquid-crystalline to crystalline phase for the Sil-ODA₁₈ sorbent increased within the T range of 303–313 K, whereas above 313 K, the ratio of the isotropic to liquid-crystalline phase increased. The decreases in phase organization followed the order of crystalline > liquid-crystalline > isotropic. Furthermore, the phase transition T gradually shifted to a higher value with a higher percentage(s) of water. These results indicated that the polarity of the mobile phase had a significant influence on the orientation order of the immobilized, silica-supported, comb-shaped nonpolar phase.

Retention Behavior of Nonpolar Solute Molecules on the Sil-ODA₁₈ Columns. Figure 3a shows the typical retention behavior of hydrocarbons on the Sil-ODA₁₈ sorbent. A distinct minimum was apparent in the plot of k' versus T for dodecane and cyclododecane, followed by an increase in retention over the T range that approximated the mesophase region. Because of the relatively small changes in the magnitude of the dead time, t_0 , or phase ratio, Φ , of the column as T was changed for a fixed mobile-phase composition, these substantial variations in k' as a function of T must reflect the reorganization of the stationary-phase surface from the crystalline to the liquid-crystalline and finally to the isotropic structure. Cycloheptane, heptane, and adamantane also showed similar retention behavior as T was increased with an increase in the k' values in the mesophase range. The k' values of these analytes increased until T reached isotropic conditions (i.e., overall, the retention of these nonpolar solutes increased over the transition range between the crystalline-to-liquid-crystalline and the liquid-crystalline-to-isotropic states. With further increases in T , the retention decreased as the isotropic state of the immobilized ligands progressively approximated an expanded liquid. In common with other studies exploring the origin of the retention processes in RPC with conventional types of n -octadecylsilica-based sorbents, the question naturally arises about the influence of the silica gel on the retention behavior of nonpolar analytes with this Sil-ODA₁₈ stationary phase. Consequently, the performance of the Sil-ODA₁₈ phase was compared using silica gels from

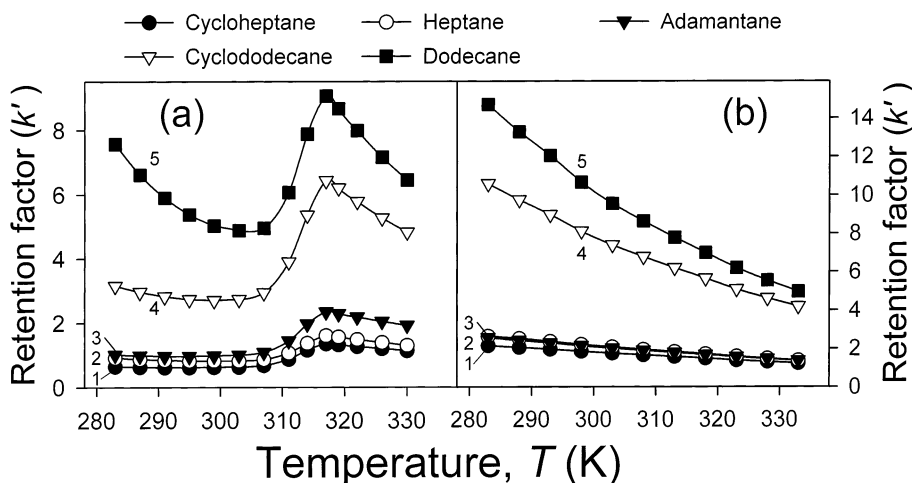


Figure 3. Comparative plots of the retention factor, k' , versus temperature, T , for (a) the Sil-ODA₁₈ sorbent and (b) the Inertsil *n*-octadecylsilica sorbent using the following solutes: 1, cycloheptane; 2, heptane; 3, adamantane; 4, cyclododecane; and 5, dodecane. The mobile phase was methanol/water (80:20 v/v), and the flow rate was 1 mL min⁻¹.

different manufacturers (e.g., YMC, Inertsil, Fuji Silysia) and with different particle/pore sizes and surface areas. Following surface modification, the carbon loading was found, as expected, to vary depending upon the type of silica gels used. For example, the carbon loadings for the YMC (5 μ m, 120 Å, 295 m² g⁻¹), Inertsil (5 μ m, 100 Å, 300 m² g⁻¹), Fuji Silysia (5.7 μ m, 115 Å, 335 m² g⁻¹), Fuji Silysia (10 μ m, 150 Å, 117 m² g⁻¹) sorbents were 16.37, 17.05, 7.5, and 12.35%, respectively. However, all of the examined analytes exhibited very similar retention behavior as T was varied with these Sil-ODA₁₈-modified sorbents to that shown in Figure 3a. Equally relevant was that the retention behavior of these Sil-ODA₁₈-modified sorbents was characteristically different from that observed for the corresponding silica sorbent modified to comparable coverage by conventional procedures with monochloro-*n*-octadecyldimethylsilane. Although it is well known that the performance of conventional *n*-octadecylsilica sorbents greatly depends on the properties of the silica gel and the type of bonding chemistry employed in their manufacture, the above results suggest that the influence of silica gel properties per se on the specific interaction of solutes with Sil-ODA₁₈-modified sorbents is largely eliminated through application of our novel surface chemistry with comb-shaped polymers such as ODA₁₈.

The type of dependence of k' on T with the Sil-ODA₁₈ sorbent has been previously observed with nonpolar analytes with liquid-crystalline phases in gas chromatography.²¹ Previous studies on liquid-crystalline phases in liquid chromatography have not, however, shown similar patterns of retention behavior with increases in k' values of nonpolar analytes with increasing T .^{22–24} These patterns of retention behavior with nonpolar solutes appear to reflect a unique attribute of Sil-ODA_n-based sorbents (where n is the number of octadecylacryl groups). In comparison, the k' values of the same nonpolar solutes with a conventional C₁₈ reversed-phase sorbent, such as the Inertsil ODS, showed monotonic decreases with increasing T (Figure 3b). These latter results are consistent with numerous, other reports on the T dependence of nonpolar solutes with similar types of monolayer *n*-alkylsilica sorbents.

Effects of Solvent and Molecular Shape or Size of Nonpolar Solutes on k' Values with Sil-ODA₁₈. In initial investigations (Figure 3a), we observed that the T value at which the k' -value increases became evident was dependent on the shape and the size of the molecule as well as on the composition of the mobile phase. It is important to note here that the magnitudes of the increases in the k' values for the smaller

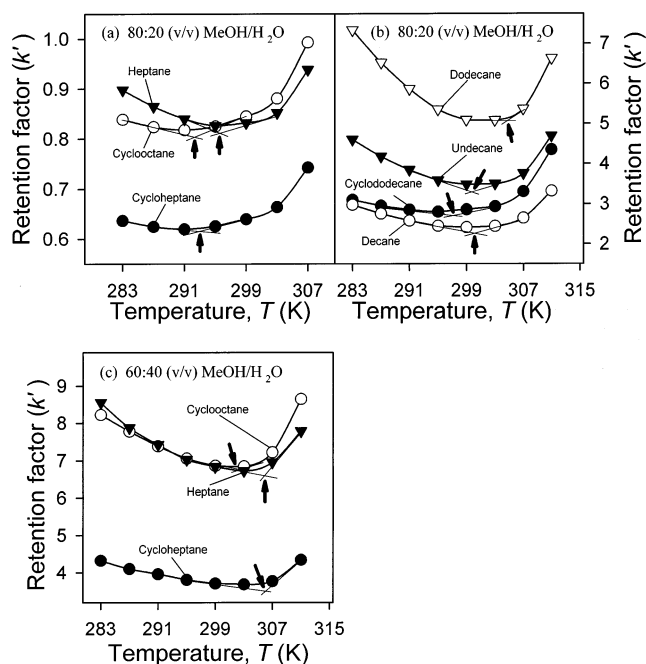


Figure 4. Plots of the retention factor, k' , for heptane, cycloheptane, cyclooctane, decane, cyclododecane, undecane, and dodecane as a function of T using the Sil-ODA₁₈ sorbent at different mobile-phase compositions, illustrating the threshold temperature condition (indicated by the arrow) at which an increase in the k' values of these solute molecules occurs. The solvent conditions used were as follows: (a) 80% (v/v) methanol/water; (b) 80% (v/v) methanol/water; and (c) 60% (v/v) methanol/water at a flow rate of 1 mL min⁻¹. The position of the threshold temperature (indicated by an arrow) was derived from the intercept of the linear regression analysis of the descending and ascending components of these plots, which depends on the shape and size of the solute molecules as well as the mobile-phase compositions.

hydrocarbons in the 80% (v/v) methanol/water mobile-phase system were relatively small (Figure 4). Hence, several additional experimental precautions were taken to ensure precision, reproducibility, and robustness in the acquisition of these data. Thus, (i) sparging of the mobile phase with helium was discontinued at the commencement of the instrumental measurement of each set of retention data since this could gradually cause changes the mobile-phase composition; the solvent was, however, sonicated at different intervals to remove any gradually dissolved air gases; (ii) the column and mobile phase were allowed to equilibrate at the same defined T for at least 30 min before going to the next injection; (iii) the retention times of

TABLE 1: Retention Factor (k') Values of the Nonpolar Solutes Measured with the Sil-ODA₁₈ Sorbent and a Mobile Phase of MeOH–H₂O

solutes	temperature, $T(K)$									
	283	287	291	295	299	303	307	311	315	317
				k'						
cycloheptane 80% (v/v) MeOH	0.637	0.625	0.620	0.626	0.640	0.664	0.743	0.947	1.239	1.325
cyclooctane 80% (v/v) MeOH	0.839	0.824	0.818	0.825	0.845	0.881	0.993	1.281	1.697	1.876
cyclododecane 80% (v/v) MeOH	3.103	2.956	2.855	2.802	2.860	2.936	3.309	4.352	5.896	6.244
<i>n</i> -heptane 80% (v/v) MeOH	0.898	0.865	0.840	0.826	0.832	0.852	0.938	1.174	1.485	1.575
<i>n</i> -decane 80% (v/v) MeOH	2.980	2.758	2.583	2.452	2.416	2.444	2.651	3.323	4.241	4.448
<i>n</i> -undecane 80% (v/v) MeOH	4.607	4.183	3.848	3.591	3.484	3.504	3.759	4.694	5.983	6.244
<i>n</i> -dodecane 80% (v/v) MeOH	7.344	6.528	5.867	5.354	5.093	5.087	5.367	6.632	8.418	8.741
cycloheptane 60% (v/v) MeOH	4.324	4.101	3.962	3.810	3.711	3.687	3.773	4.343	6.111	7.090
cyclooctane 60% (v/v) MeOH	8.226	7.783	7.390	7.058	6.866	6.849	7.224	8.650	13.237	15.474
<i>n</i> -heptane 60% (v/v) MeOH	8.555	7.877	7.425	7.029	6.841	6.728	6.956	7.787	10.511	11.850

the various analytes were measured with single injections of the mixtures, repeated at least in triplicate, where peaks overlapped with a particular mobile-phase composition, and then each of the analytes was injected sequentially; (iv) the temperature of the column and mobile phase was uniformly controlled throughout the experiment; and (v) statistically relative retention and resolution map procedures were used to ensure that the system was stable and satisfied the criteria of “reversible, near-equilibrium”. The column dead time, t_0 , and dead volume, V_0 , were measured after every fourth injection to accommodate any small changes in values as the T was increased, and these values were taken into account in the calculation of the k' values.

Utilizing these carefully controlled techniques, it was feasible to determine accurately the T values at which the k' increased, with these increases in k' values occurring at the T values indicated by the arrows in Figure. 4. Thus, in 80% (v/v) methanol/water above ~ 295 K, cycloheptane and cyclooctane showed an increase in k' with increasing T , whereas from ~ 299 K, the linear analogue heptane (Figure 4a) showed analogous behavior. Similarly, cyclododecane exhibited k' increases in 80% (v/v) methanol/water at $T \approx 299$ K with the Sil-ODA₁₈ sorbent, whereas analogous behavior was observed at $T \approx 303$ K for undecane and decane and at $T \approx 307$ K for dodecane (Figure 4b). In 80% (v/v) methanol/water cyclopentane, cyclohexane and cyclodecane showed an increase in k' values at $T \approx 295$ K, whereas comparable behavior was observed at $T \approx 299$ K for hexane, octane, and nonane. When the water content of the mobile phase was increased, the T -value thresholds leading to increases in the k' values with the Sil-ODA₁₈ sorbent shifted to higher values. Thus, the T value at which increases in the k' values was evident for cycloheptane, cyclooctane, and heptane in 60% (v/v) methanol/water shifted to ≥ 307 K (Figure 4c). The retention data with the Sil-ODA₁₈ sorbent for cycloheptane, cyclooctane, cyclododecane, heptane, decane, undecane, and dodecane in 80% (v/v) methanol/water or 60% (v/v) methanol/water are shown in Table 1, with the k' values at which increases occurred with increasing T highlighted in bold. As is apparent from these results, as the volume fraction of methanol was increased, the k' values of the solutes decreased. Concomitant with this trend is that as the volume fraction of methanol was increased the transition to higher k' values occurred at lower T values. Thus, the T value at which k' values increased for cyclohexane with the Sil-ODA₁₈ sorbent shifted from $T \approx 303$ K for the 60% (v/v) methanol/water mobile phase to $T \approx 307$ K with 50% (v/v) methanol/water. Rigid polycyclic compounds such as adamantane, tricyclene, and *trans*-pinane also exhibited k' increases above $T \approx 295$ K in 80% (v/v) methanol/water, and likewise the T values at which the k' values shifted occurred at higher values with mobile phases of increasing water content. The retention behavior of these analytes was investigated down to 30% (v/v) methanol/water with the Sil-ODA₁₈ sorbent. The

different solute molecules, particularly the nonplanar cyclic and open-chain *n*-alkanes, showed k' increases at $T \approx 307$ K even at this higher water content. Finally, these T dependencies were also investigated using 90% (v/v) methanol/water, with the retention behavior of these solute molecules found to be similar to that obtained with 80% (v/v) methanol/water. From a mechanistic perspective, these investigations emphasize the importance of the molecular size and structure of these nonpolar solutes in their interactions with this new Sil-ODA₁₈ sorbent, with the dependencies of k' on T collectively indicating a transition from an enthalpy-driven to an entropy-driven process. Such processes have been widely observed previously in protein solvation phenomena and in protein-folding pathways and have also been associated with the interaction of protein ligands with their cognate binding partners.^{19,20,25–29} Moreover, the results shown in Figures 3a and 4a and b, in particular, emphasize the importance of group molecular parameters (GMPs), which can be expressed in terms of the nonpolar surface contact areas that these nonpolar molecules establish with the immobilized ligands of the stationary phase and their linkage to linear free-energy dependencies and shape-selectivity parameters. From these viewpoints, these retention data provide useful bases to examine the interaction thermodynamics of these nonpolar solutes with this sorbent at the molecular level.

Determination of the Interaction Thermodynamic Parameters for Heterothermic Processes with the Sil-ODA₁₈ Sorbent. The reversible, near-equilibrium criterion is generally assumed to prevail for the binding and subsequent desorption of low-molecular-weight compounds with RPC sorbents. Changes in thermodynamic parameters due to solute association with the immobilized ligands can then be described in terms of the Gibbs–Helmholtz relationship:

$$\Delta G_{\text{assoc}}^{\circ} = \Delta H_{\text{assoc}}^{\circ} - T\Delta S_{\text{assoc}}^{\circ} \quad (1)$$

When such conditions prevail, the interaction thermodynamics of the solute molecules, surrounding bulk, structured solvent, and solvated nonpolar surface of the sorbent are often assumed to be invariant with regard to T . Hence, contributions of the corresponding changes in enthalpy, $\Delta H_{\text{assoc}}^{\circ}$, and entropy, $\Delta S_{\text{assoc}}^{\circ}$, to the change in the Gibbs free energy, $\Delta G_{\text{assoc}}^{\circ}$, associated with solute–sorbent interaction will also be independent of T . When such conditions are achieved, the dependence of the logarithm of the retention factor, $\ln k'$, on $1/T$ takes the form of a linear van't Hoff plot. The interaction of solutes with the nonpolar surface of an RP-HPLC sorbent can then be described by the following expression:

$$\ln k' = -\Delta H_{\text{assoc}}^{\circ}/RT + \Delta S_{\text{assoc}}^{\circ}/R + \ln \Phi \quad (2)$$

where R is the gas constant and Φ is the phase ratio of the

system. Provided the phase ratio and structural properties of the solute and sorbent surface are invariant with T , the values of $\Delta H_{\text{assoc}}^{\circ}$ and $\Delta S_{\text{assoc}}^{\circ}$ can be derived from eq 2 in the traditional manner by linear regression analysis of the $\ln k'$ versus $1/T$ plots as the slope and intercept values, respectively. Although linear van't Hoff plots have been observed^{8,10,17} for some low-molecular-weight molecules in RPC, significant divergence from linearity has been noted when nonpolar ligands immobilized onto a stationary phase undergo a phase transition or alternatively when the solutes themselves undergo a structural change on binding. In particular, nonlinear behavior in the van't Hoff plots is often observed in RPC systems for peptides or proteins.^{19,20,25–29} This behavior is usually attributed to changes in the secondary or tertiary structure of these molecules, arising from the perturbing effects of the aquo-organic solvent mobile phase or from the interaction with the hydrocarbonaceous sorbent.

To gain further insight into the basis of solute–nonpolar ligand interactions with the Sil-ODA₁₈ sorbent, various thermodynamic parameters associated with the test group of nonpolar solutes were determined on the basis of an approach^{20,26–28} recently introduced to evaluate physicochemical/biophysical parameters of polypeptides and other hydrophobic molecules from nonlinear van't Hoff plots. Previously, the inability to determine the phase ratio precisely has led to difficulties in evaluating the corresponding thermodynamic values. Although several approaches for the measurement of Φ can be found^{26,27} in the literature, some disagreement still remains on the preferred procedure. In this new approach, the contribution of the phase ratio to the retention factor, k' , can also be accommodated, providing greater precision in the determination of the changes in the enthalpy, entropy, and heat capacity of the system.

In the bulk state, the standard heat capacity, C_p° , of a substance is defined as the quantity of heat necessary to raise the T value of a unit mass of the substance by one degree Kelvin. In the case of RPC systems, three situations can be contemplated for the interaction of solutes with the immobilized ligands, whereby the change in heat capacity, ΔC_p° , of the system (i) is zero and remains invariant with regard to T (i.e., an isothermic scenario); (ii) is not zero but is linearly dependent on T (i.e., a homothermic scenario); or (iii) is not zero and shows a nonlinear dependence on T (i.e., a heterothermic scenario).^{19,20,26–31} According to the Kirchoff relationships,^{32,33} the change in the heat capacity, ΔC_p° , for a solute-immobilized nonpolar ligand-interactive system as a function of T can be expressed in terms of eq 3–7 as

$$\Delta C_p^{\circ} = T \partial S_{\text{assoc}}^{\circ} / \partial T \quad (3)$$

$$\Delta S_{\text{assoc}}^{\circ} = \int (\Delta C_p^{\circ} / T) dT \quad (4)$$

$$\Delta C_p^{\circ} = \partial H_{\text{assoc}}^{\circ} / \partial T \quad (5)$$

$$\Delta H_{\text{assoc}}^{\circ} = \int \Delta C_p^{\circ} dT \quad (6)$$

$$\Delta C_p^{\circ} \partial T = \partial E + P \partial V - \mu_i \partial \mu_i \quad (7)$$

where ∂E represents the incremental difference in the internal energy of the system. Thus, ΔC_p° is related to the change in the standard enthalpy and the standard pressure–volume product (∂PV), whereas the term μ_i takes into account contributions from processes not defined by the Stefan–Boltzmann–Maxwell law. If the interaction does not involve any effects other than standard

changes in P , V , and T , then eq 7 becomes

$$\Delta C_p^{\circ} \partial T = \partial E + P \partial V \quad (8)$$

$$\Delta C_p^{\circ} \partial T = \partial H_{\text{assoc}}^{\circ} - \partial(PV) + P \partial V \quad (9)$$

and hence

$$\Delta C_p^{\circ} \partial T = \partial H_{\text{assoc}}^{\circ} - V \partial P \quad (10)$$

If the heat capacity of the system is increased under experimental conditions whereby P does not change significantly, then eq 10 can be simplified, and the specific heat capacity can be redefined as follows:

$$C_p^{\circ} = (\partial H_{\text{assoc}}^{\circ} / \partial T)_P \quad (11)$$

Equations 3–11 provide a useful framework to assess the interaction between solutes and immobilized nonpolar ligands, enabling the relationship between $\ln k'$, T , and the thermodynamic parameters $\Delta H_{\text{assoc}}^{\circ}$, $\Delta S_{\text{assoc}}^{\circ}$, and ΔC_p° to be evaluated for a defined solute, flow rate, and mobile-phase composition. In the present studies with the Sil-ODA₁₈ sorbent, these relationships were validated for isocratic systems in the range of $T = 278$ to 343 K at a pressure of ~ 220 – 240 bar.

The dependence of the equilibrium association constant, K_{assoc} , for the interaction of a solute with the immobilized nonpolar ligands as a function of T takes the form

$$K_{\text{assoc}} = e^{-\Delta G_{\text{assoc}}^{\circ} / RT} \quad (12)$$

where the Gibbs free energy change for the interaction, $\Delta G_{\text{assoc}}^{\circ}$, is a function of T only. By substituting and rearranging the relevant terms, the following thermodynamic dependencies can be derived:

$$\partial \ln K_{\text{assoc}} = -1/R[(T \partial G_{\text{assoc}}^{\circ} / T^2)] \quad (13)$$

$$\partial \ln K_{\text{assoc}} / \partial T = \Delta H_{\text{assoc}}^{\circ} / RT^2 \quad (14)$$

where the equilibrium association constant, K_{assoc} , for the binding of the solute to the immobilized nonpolar ligand is related to the retention factor, k' , through the relationships

$$\ln K_{\text{assoc}} = \ln k' + \ln \Phi \quad (15)$$

$$\partial \ln k' / \partial T = \Delta H_{\text{assoc}}^{\circ} / RT^2 \quad (16)$$

When both $\Delta H_{\text{assoc}}^{\circ}$ and $\Delta S_{\text{assoc}}^{\circ}$ are invariant with T (i.e., isothermic binding conditions prevail), linear van't Hoff plots are observed, and the following expression is obtained:

$$\ln k' = -\Delta H_{\text{assoc}}^{\circ} / RT + I \quad (17)$$

where $I = -\Delta S_{\text{assoc}}^{\circ} / R + \ln \Phi$. If the phase ratio is independent of T , then the plot of $\ln k'$ versus $1/T$ will be a straight line, characteristic of linear van't Hoff plots. Data derived from several studies have demonstrated that changes in Φ at specified solvent composition are usually small (i.e., $\leq \pm 10\%$) over the examined T range when n -alkylsilicas are used, suggesting that the contribution of the $\ln \Phi$ term to the $\ln k'$ values will be small and essentially constant.

When $\Delta H_{\text{assoc}}^{\circ}$ and $\Delta S_{\text{assoc}}^{\circ}$ are, however, dependent on T , the plots of $\ln k'$ versus $1/T$ do not follow linear dependencies. When the T -dependent heat capacity condition prevails (i.e., $\Delta C_p^{\circ} \neq 0$), then the dependence of $\ln k'$ on T can be approximated by

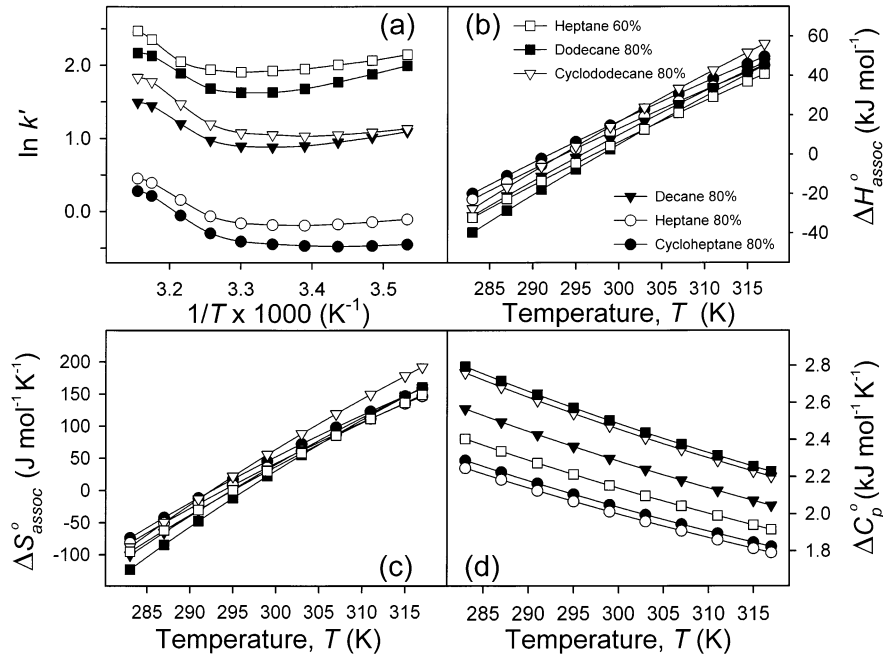


Figure 5. Typical van't Hoff plots illustrating the dependence of $\ln k'$ on $1/T$, derived for several solutes with the Sil-ODA₁₈ sorbent from the retention data given in Table 1. In panel (a) are shown the $\ln k'$ versus $1/T$ plots for heptane, cycloheptane, decane, dodecane, and cyclododecane in 80% (v/v) methanol/water and heptane in 60% (v/v) methanol/water. In panels (b), (c), and (d) are shown, respectively, the dependencies of $\Delta H^\circ_{\text{assoc}}$, $\Delta S^\circ_{\text{assoc}}$, and ΔC°_p on $T(K)$ based on the data shown in Tables 1 and 2.

the polynomial expression

$$\ln k' = a + b(1/T) + c(1/T)^2 + d(1/T)^3 + \dots + \ln \phi \quad (18)$$

and thus

$$\partial \ln k' / \partial T = [\partial \ln k' / \partial (1/T)] [\partial (1/T) / \partial T] \quad (19)$$

$$= -(1/T)^2 [b + 2c(1/T) + 3d(1/T)^2 + \dots] \quad (20)$$

When such homothermic and heterothermic scenarios prevail, the change in enthalpy can thus be represented by

$$\Delta H^\circ_{\text{assoc}} = -R[b + 2c(1/T) + 3d(1/T)^2 + \dots] \quad (21)$$

whereas the change in heat capacity can be represented by

$$\Delta C^\circ_p = \partial \Delta H^\circ_{\text{assoc}} / \partial T \quad (22)$$

$$= m/(T)^2 + n/(T)^3 + \dots \quad (23)$$

where $m = 2Rc$ and $n = 6Rd$, etc.

Since the slope of the plot of $\ln k'$ versus $1/T$ at any T value will be proportional to the $\Delta H^\circ_{\text{assoc}}$ value at that T value,³⁴ the value of $\Delta H^\circ_{\text{assoc}}$ can reach zero at a unique $\ln k'$ value specified by the temperature, T_H . In such circumstances and when ΔC°_p is constant, the dependence of $\Delta H^\circ_{\text{assoc}}$ and $\Delta S^\circ_{\text{assoc}}$ can be expressed in terms of ΔC°_p as

$$\Delta H^\circ_{\text{assoc}} = \Delta H^*_{\text{assoc}} + \Delta C^\circ_p (T - T^*_H) \quad (24)$$

$$\Delta S^\circ_{\text{assoc}} = \Delta S^*_{\text{assoc}} + \Delta C^\circ_p \ln(T/T^*_S) \quad (25)$$

where T^*_H and T^*_S refer to the isoenthalpic and isentropic temperatures at which the plots of $\Delta H^\circ_{\text{assoc}}$ versus T and $\Delta S^\circ_{\text{assoc}}$ versus T , respectively, for the solute(s) intercept and attain a common value of $\Delta H^*_{\text{assoc}}$ and $\Delta S^*_{\text{assoc}}$ under the

different experimental conditions. When such solute-immobilized nonpolar ligand binding processes occur, the dependence of $\ln k'$ on T can be approximated³⁵ by

$$\ln k' = \Delta C^\circ_p / R [T_H/T - \ln(T_S/T) - 1] + \ln \Phi \quad (26)$$

Thus, derivation of the values of $\Delta H^\circ_{\text{assoc}}$, $\Delta S^\circ_{\text{assoc}}$, and ΔC°_p using nonlinear least-squares regression methods and associated curve-fitting procedures with the Hephaestus and Eudoxos software packages^{27,28} can provide significant information on whether the retention behavior is characterized by homothermic and heterothermic interaction processes. This method has recently been validated^{19,25–30} with peptides and proteins in both reversed-phase and hydrophobic interaction high-performance liquid chromatography. Moreover, these studies have indicated that the partial molar volumes, v_p , of peptides and proteins vary only to a very small extent (i.e., $< 5\%$) in the pressure range of ~ 220 – 250 bar, and even smaller changes in v_p were predicted to occur for small organic molecules such as the test set of n -alkanes and cycloalkanes, under the operational range of these experiments. We have now applied this approach to evaluate the interaction thermodynamics of the test set of n -alkanes and cycloalkanes with the Sil-ODA₁₈ sorbent and have compared these results to the data obtained with a conventional n -alkylsilica sorbent.

The $\ln k'$ versus $1/T$ plots for cycloheptane, heptane, decane, cyclododecane, and dodecane (Figure 5a) represent typical examples of the van't Hoff dependencies of these nonpolar solutes where the Sil-ODA₁₈ sorbent predominantly exhibits a single state. The corresponding values of $\Delta H^\circ_{\text{assoc}}$, $\Delta S^\circ_{\text{assoc}}$, and ΔC°_p determined for cycloheptane, heptane, decane, cyclododecane, and dodecane from these plots (Figure 5b–d) over the T range from 283 to 317 K are provided in Table 2. As is apparent from these results, the $\Delta H^\circ_{\text{assoc}}$ values for cycloheptane, heptane, decane, cyclododecane, and dodecane in 80% (v/v) methanol/water were exothermic at low T values but

TABLE 2: Thermodynamic Parameters Derived for the Various Nonpolar Solutes Measured with the Si-ODA₁₈ Sorbent over the Temperature Range of 283–317 K

solutes		temperature, <i>T</i> (K)									
		283	287	291	295	299	303	307	311	315	317
cycloheptane 80% (v/v) MeOH	$\Delta H_{\text{assoc}}^{\circ}$	−19.9	−10.9	−2.1	6.5	14.8	22.9	30.7	38.4	45.9	49.6
	$\Delta S_{\text{assoc}}^{\circ}$	−73.6	−41.9	−11.6	17.6	45.5	72.4	98.2	123.1	147.0	158.6
	ΔC_p°	2.3	2.2	2.2	2.1	2.1	2.0	1.9	1.9	1.8	1.8
cyclododecane 80% (v/v) MeOH	$\Delta H_{\text{assoc}}^{\circ}$	−27.7	−16.8	−6.2	4.1	14.1	23.9	33.4	42.6	51.7	56.1
	$\Delta S_{\text{assoc}}^{\circ}$	−88.0	−49.8	−13.2	22.0	55.7	88.1	119.3	149.3	178.1	192.1
	ΔC_p°	2.8	2.7	2.6	2.5	2.5	2.4	2.3	2.3	2.2	2.2
<i>n</i> -heptane 80% (v/v) MeOH	$\Delta H_{\text{assoc}}^{\circ}$	−22.9	−14.0	−5.4	3.0	11.1	19.1	26.8	34.4	41.7	45.3
	$\Delta S_{\text{assoc}}^{\circ}$	−81.3	−50.2	−20.4	8.2	35.6	62.0	87.4	111.8	135.2	146.6
	ΔC_p°	2.2	2.2	2.1	2.1	2.0	2.0	1.9	1.9	1.8	1.8
<i>n</i> -heptane 60% (v/v) MeOH	$\Delta H_{\text{assoc}}^{\circ}$	−32.2	−22.7	−13.5	−4.5	4.2	12.7	21.0	29.0	36.9	40.8
	$\Delta S_{\text{assoc}}^{\circ}$	−95.3	−62.1	−30.2	0.4	29.8	58.0	85.1	111.2	136.3	148.5
	ΔC_p°	2.4	2.3	2.3	2.2	2.2	2.1	2.0	2.0	1.9	1.9
<i>n</i> -decane 80% (v/v) MeOH	$\Delta H_{\text{assoc}}^{\circ}$	−31.2	−21.1	−11.2	−1.7	7.7	16.7	25.6	34.2	42.6	46.7
	$\Delta S_{\text{assoc}}^{\circ}$	−100.7	−65.2	−31.2	1.5	32.9	63.0	92.0	119.8	146.6	159.7
	ΔC_p°	2.6	2.5	2.4	2.4	2.3	2.2	2.2	2.1	2.1	2.0
<i>n</i> -dodecane 80% (v/v) MeOH	$\Delta H_{\text{assoc}}^{\circ}$	−39.7	−28.7	−17.9	−7.5	2.6	12.5	22.1	31.5	40.7	45.1
	$\Delta S_{\text{assoc}}^{\circ}$	−123.1	−84.4	−47.4	−11.8	22.4	55.2	86.7	117.0	146.2	160.4
	ΔC_p°	2.8	2.7	2.6	2.6	2.5	2.4	2.4	2.3	2.3	2.2

became endothermic at the higher *T* values (Figure 5b). Concomitantly, the $\Delta S_{\text{assoc}}^{\circ}$ values became progressively larger and more positive (Figure 5c), whereas the ΔC_p° values for all of these solutes became smaller (Figure 5d).

Origin of the *k'*-Value Increases of the Nonpolar Solutes on the Si-ODA₁₈ Sorbent. Participation of the “hydrophobic effect” is usually associated with *T*-dependent solvational phenomena when a nonpolar solute is transferred into water, revealing a minimum in solubility for hydrocarbons in water at or near room *T* (i.e., near 298 K).^{32,36–40} A minimum in the solubility of a nonpolar solute often corresponds to a maximal retention in RPC.¹¹ This *T* dependence arises from the ordering of water molecules around the small nonpolar solutes. The extent of this solvation is often used as a measure of the “hydrophobicity” of the solutes. The ordering of water molecules around small nonpolar solutes is most effective at 298 K and decreases as *T* is increased. At 298 K, the hydrophobic effect is entropically driven, whereas at high *T* (e.g., *T* = 415 K), it becomes enthalpically controlled.³² This narcissian “disaffinity” or repugnance of nonpolar solutes for cold water (at room *T* or below) is due to the nature of the ordering of the neighboring water molecules (i.e., entropic effects), whereas the disaffinity for hot water is largely due to the breaking of hydrogen bonds among the neighboring water molecules (i.e., enthalpic effects).³⁹ Since small nonpolar solutes are strongly expelled from water at room *T* onto nonpolar surfaces, maximum chromatographic retention should be observed at or near this *T* value. Cole et al.¹¹ observed a maximum *k'* value at 293 K for benzene with *n*-octadecylsilica sorbents when 95% water/1-propanol mixtures were used as the eluent. However, as evident from Figure 3 with the Si-ODA₁₈ sorbent, the maximum retention of several *n*-alkanes, cycloalkanes, and polycyclic hydrocarbons occurred near *T* = 318 K, with the shape of the *k'* versus *T* dependence distinctly different between the Si-ODA₁₈ and *n*-octadecylsilica sorbent. This pattern of *k'*–*T* dependencies with the Si-ODA₁₈ phase arises from the stationary-phase contribution as the phase undergoes a transition from the crystalline to the noncrystalline state. We also observed that this retention maximum gradually moved to higher *T* values as the percentage of water was increased (i.e., with increasing polarity of the solvent, the phase-

transition *T* value shifted to higher values, as evident also from the DSC measurements; cf. Figures 3a and 2). Thus, the operational range of the crystalline state of the Si-ODA₁₈ phase increased with mobile phases of higher water content. This finding indicates that the Si-ODA₁₈ phase becomes more ordered as the mobile-phase polarity is increased.

Statistical mechanical modeling of the *n*-alkyl-based RPC sorbents has shown that the insertion of nonpolar solutes into an already constrained *n*-alkyl chain can cause the solute–ligand complex to become more ordered, resulting in an entropically driven effect that opposes further solute insertion,⁴¹ whereas a hydrophobic entropic effect (associated with the ordering of water molecules around the nonpolar solutes) opposes solute insertion into water. In accordance with these observations, the nonpolar solutes with the Si-ODA₁₈ sorbent followed nearly linear dependencies of $\Delta H_{\text{assoc}}^{\circ}$ and $\Delta S_{\text{assoc}}^{\circ}$ on *T* (Figure 5b and c). At low *T* values, $\Delta H_{\text{assoc}}^{\circ}$ was <0 (i.e., the binding process was exothermic) for the Si-ODA₁₈ phase in the crystalline state but became positive as the phase underwent a transition to the noncrystalline state (Table 2).

These findings support the conclusion that the retention of nonpolar solutes is an energetically more favorable process when the Si-ODA₁₈ sorbent is in the crystalline rather than the noncrystalline state. The $\Delta S_{\text{assoc}}^{\circ}$ values for these solutes were negative in the range of *T* values corresponding to the Si-ODA₁₈ sorbent in the crystalline state but became positive with increasing *T* (Figure 5c and Table 2). The reverse situation was observed with the conventional *n*-octadecylsilica sorbent. With conventional C₁₈ silica sorbents of different ligand densities, Cole et al.¹¹ have also observed positive $\Delta S_{\text{assoc}}^{\circ}$ values for the interaction of nonpolar solutes such as benzene at or below room *T* (i.e., 298 K or below) using 95% (v/v) water/1-propanol as the mobile phase, whereas $\Delta S_{\text{assoc}}^{\circ}$ became negative at higher *T* values. Positive values of $\Delta S_{\text{assoc}}^{\circ}$ indicate a decrease in the order of the system for the transfer of a nonpolar solute from a polar mobile phase to the nonpolar C₁₈ sorbent. However, when nonpolar solute transfers back to the bulk liquid state of the mobile phase, the entropy changes at 298 K are negative but become positive with increasing *T*. A decrease in entropy at

298 K for the transfer of a nonpolar solute from a less polar to a more polar liquid is one of the signatures of the hydrophobic effect.^{32,37–40} Since the opposite process is evaluated in chromatographic systems, Cole et al.¹¹ concluded that the positive $\Delta S_{\text{assoc}}^{\circ}$ value for benzene at 298 K and a decrease in the magnitude of $\Delta S_{\text{assoc}}^{\circ}$ as T was increased were evidence of the participation of the hydrophobic effect. Additionally, Cole et al.⁸ found that the change in entropy at any given T for nonpolar solutes was greater with low-density C_{18} sorbents than with high-density C_{18} sorbents with such mobile-phase systems. This finding indicates that a greater repulsion occurred from the higher-density C_{18} sorbent than from the lower-density C_{18} sorbent, consistent with the interphase theory of retention predicted by Dill.^{4,5,41} Negative $\Delta S_{\text{assoc}}^{\circ}$ values for nonpolar solutes with n - C_{18} silica sorbents were also obtained¹¹ when acetonitrile/water was used as the mobile phase, with the change in entropy becoming more positive as the stationary-phase bonding density was increased, a finding in conflict with the interphase theory of retention.

A decrease in entropy for solutes in RPC has been used as evidence of the interphase nature of nonpolar stationary phases, demonstrating the difference between a partially ordered interphase and a bulk system. The transfer of solutes into the grafted chains of an n -alkylsilica in fact depends on the entropy of mixing, the configuration of the chains, and the interaction of solutes with the chains.⁴¹ Therefore, to probe the sign as well as magnitude (i.e., decrease or increase) of the $\Delta S_{\text{assoc}}^{\circ}$ values with the Sil-ODA₁₈ sorbent system, attention was given to the nature of the ordering of the stationary phase. In the chromatographic context of solute–ligand association, a decrease or increase in entropy is a relative concept. The evaluation of the contribution of entropy to the association thermodynamics of nonpolar solutes with the Sil-ODA₁₈ sorbent was thus considered from the perspective of two relative aspects, namely, solute exclusion at higher T values and chain ordering. The observed negative $\Delta S_{\text{assoc}}^{\circ}$ values at low T values for the various hydrocarbons used in the current studies with the Sil-ODA₁₈ sorbent reflect an increase in the order of the system when these solutes are transferred from the polar (methanol/water) environment to the nonpolar environment of the Sil-ODA₁₈ phase in the crystalline state.

DeVido and co-workers¹⁷ have recently envisioned a possible partition mechanism for solutes at high and low T into a grafted n -alkyl chain sorbent system, which is pertinent to high-density C_{18} stationary phases. According to this model, at low T , the solute partitions closer to the grafted end of the n -alkyl chain, with the partition process favored by the changes in enthalpy but opposed by the entropy changes. However, at high T values, the solutes are squeezed from the stationary-phase surface toward the chain ends with the entropy effects progressively becoming dominant over the enthalpy effects. Partitioning of the nonpolar solutes into the Sil-ODA₁₈ phase between 291 to 318 K can thus be envisioned to occur in a similar way (i.e., the entropic contributions become significant as T increases), whereas enthalpic effects will dominate over entropic effects at T values below 291 K. At low T values, the nonpolar solutes will have tight contact with chains because of the favorable enthalpy change (negative $\Delta H_{\text{assoc}}^{\circ}$), but this tight contact will be opposed by the entropy change associated with the chain ordering. Penetration of the solutes into the chains of the Sil-ODA₁₈ phase in the crystalline state (i.e., below 291 K) will thus be an entropically less-favorable process. The negative values of $\Delta S_{\text{assoc}}^{\circ}$ thus indicate an entropic repulsion of the

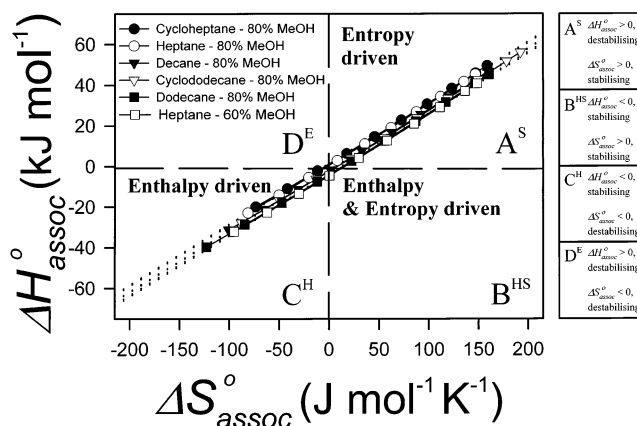


Figure 6. Entropy–enthalpy compensation relationship between $\Delta S_{\text{assoc}}^{\circ}$ and $\Delta H_{\text{assoc}}^{\circ}$ based on the experimental data given in Table 2 for heptane, cycloheptane, decane, dodecane, and cyclododecane in 80% (v/v) methanol/water and heptane in 60% (v/v) methanol/water. The solid lines correspond to the first-order fit of the data with the dotted lines corresponding to the 95% confidence limits.

solutes on their attempted penetration into the Sil-ODA₁₈ phase in the crystalline state.

However, at high T values, these nonpolar solutes will progressively have less-tight solute contacts with the nonpolar ligands and a less-favorable enthalpy change (positive $\Delta H_{\text{assoc}}^{\circ}$), but this process will at the same time be less opposed by the entropy change (positive $\Delta S_{\text{assoc}}^{\circ}$). Therefore, the retention of these nonpolar solutes in the crystalline state of the Sil-ODA₁₈ sorbent is largely enthalpically driven, whereas in the noncrystalline state, the dominant driving force arises mainly from the changes in entropy. Within the regions of retention behavior where a single mechanism prevails, enthalpy–entropy compensation effects can, however, arise, as illustrated by the plot of $\Delta S_{\text{assoc}}^{\circ}$ versus $\Delta H_{\text{assoc}}^{\circ}$ for cycloheptane, heptane, decane, cyclododecane, and dodecane in the presence of the Sil-ODA₁₈ sorbent in the crystalline state (Figure 6), with the compensation temperatures for these analytes calculated to be around $T = 300$ K. Compared to those of traditional RPC systems, these compensation temperature values are smaller, falling below the range of 500–1500 K calculated for many n -alkylsilica systems.

The Sil-ODA₁₈ sorbent thus provides a useful system from to gain further understanding of the origins of enthalpy–entropy compensation effects in RPC, with the results obtained with this sorbent consistent with the interphase theory of retention and with solute retention in the Sil-ODA₁₈ phase in the crystalline state depending upon how effectively the solutes are incorporated onto the ordered ligand structure. Enthalpy–entropy compensation represents an extrathermodynamic relationship that is typical for molecular interactions comprising multiple, weak intermolecular forces, whereby a linear dependence of $\Delta H_{\text{assoc}}^{\circ}$ on $\Delta S_{\text{assoc}}^{\circ}$ is observed following a change in an experimental variable such as T . These dependencies clearly demonstrate how the retention of solutes on the Sil-ODA₁₈ phase shifts from an enthalpy-driven to an entropy-driven retention process as the phase undergoes a transition from the crystalline to the noncrystalline state. The compensation temperatures, namely, T_H (where $\Delta H_{\text{assoc}}^{\circ} = 0$) and T_S (where $\Delta S_{\text{assoc}}^{\circ} = 0$), thus define these processes, irrespective of whether the interaction is driven by changes in enthalpy, entropy, or both. As depicted in Figure 6 in region A^S, $\Delta H_{\text{assoc}}^{\circ} > 0$ (destabilizing with respect of the analyte–nonpolar ligand interaction) and $T\Delta S_{\text{assoc}}^{\circ} > 0$ (stabilizing with respect of the analyte–nonpolar

ligand interaction); in region B^{HS}, $\Delta H_{\text{assoc}}^{\circ} < 0$ and $T\Delta S_{\text{assoc}}^{\circ} > 0$ (both stabilizing with respect of the analyte–nonpolar ligand interaction); and in region C^H, $\Delta H_{\text{assoc}}^{\circ} < 0$ (stabilizing with respect of the analyte–nonpolar ligand interaction) and $\Delta S_{\text{assoc}}^{\circ} < 0$ (destabilizing with respect of the analyte–nonpolar ligand interaction). An alternative graphical representation that is useful for the determination of the transition points in the dependence of k' on T is shown in Figure 4 since a change in slope of the k' versus T plots directly equates with a change in the sign of the enthalpy. Because of the well-known difficulty in the determination of the pre- and post-translational baseline in DSC, the exact measurement of T_C is somewhat arbitrary with binary ligand–solvent systems (cf. Figure 2). Since the contribution of the interacting solute cannot be directly measured in the ternary ligand–solvent–solute system by DSC procedures, regardless of whether the compensation temperatures T_H and T_S are derived from the relationships implicit to the data shown in Figures 4 and 6, by the very nature of the DSC investigations, T_H and T_S cannot be directly correlated to the compensation points T_{C1} .

As apparent from the results shown in Figure 5d, the changes in heat capacity, ΔC_p° , of the system were not zero but were linearly dependent on T . This behavior corresponds to the homothermic scenario of the solute–stationary binding process. One of the most distinctive thermodynamic signatures associated with the burial of hydrophobic solutes in a nonpolar ligand environment is a large and negative ΔC_p° value.^{42–46} The negative heat capacity arises from the dehydration of the solute upon insertion into the nonpolar environment. This is also known as the cause of the hydrophobic effect.^{42,45} The question thus arises, What significance can be ascribed to the sign of ΔC_p° in RPC systems? Negative ΔC_p° values are expected only for analytes in a highly aqueous phase system when the hydrophobic effect dominates the retention process and sufficient dehydration occurs upon burial of the analyte in the nonpolar core. In other words, the magnitude of the negative ΔC_p° should be related to the extent of burial in the nonpolar sorbent. De Vido et al.¹⁷ obtained $\Delta C_p^{\circ} = -182.4$ (J mol^{−1} K^{−1}) for the transfer of arginine from water into a low-bonding-density C₁₈ sorbent (2.41 μmol^{−2}) at 296 K, whereas with a high-bonding-density C₁₈ sorbent (4.3 μmol^{−2}), $\Delta C_p^{\circ} = 0$ (J mol^{−1} K^{−1}).¹⁷ The results of this investigator are in agreement with our prediction that less burial of this amino acid into this high-bonding-density C₁₈ sorbent can be expected. A second question also arises, What is the origin of positive ΔC_p° values observed in our present investigation? Cole and co-workers¹¹ have noted that solvophobic theory may be a reasonable explanation for a hydrogen-bonded or highly aqueous mobile phase, but solvophobic theory is not an adequate explanation for the retention behavior of other mobile-phase systems. According to Cole et al.,¹¹ solvophobic theory is less applicable to RPC retention processes with 80% methanol/water mobile-phase systems, with the retention behavior following more closely a partition processes and the heat capacity changes for nonpolar solutes becoming positive upon reduction of the hydrophobic driving force with such mobile-phase systems. Thus, the conclusion can be drawn that the positive ΔC_p° values observed for the *n*-alkanes and cycloalkanes at low T values using 80% methanol/water with Sil-ODA₁₈ sorbent arise from an unfavorable partitioning process and a weak hydrophobic driving force. In our associated studies, the nature of the temperature dependence of the interaction thermodynamics of small peptides in RPC environments using Sil-ODA₁₈ sorbents has been examined for a wide range of solvent

systems (i.e., from aqueous to highly organic mobile-phase systems). These investigations (Chowdhury, M. A. J.; Hearn, M. T. W. Unpublished observations, 2001) have revealed that the sign and the magnitudes of $\Delta S_{\text{assoc}}^{\circ}$, $\Delta H_{\text{assoc}}^{\circ}$, or ΔC_p° under different chromatographic conditions depend on the nature of the stationary-phase structure, the nature of the water structure in the mobile phase, and the magnitude of the unfolding state of the peptides.

A further effect (i.e., liquid crystallinity) determines the extent of solute penetration into the Sil-ODA₁₈ sorbent. The extent of liquid crystallinity of this sorbent increased with increasing T between 291 and 317 K in 80% (v/v) methanol/water and hence the extent of solute partitioning. When T reaches the isotropic value (i.e., above ~317 K), enthalpy–entropy compensation continues but becomes associated with decreases in retention and a simultaneous diminution of the influence of the hydrophobic effect as T increases further. Therefore, the decrease in retention of these nonpolar solutes with the sorbent in the isotropic state can be interpreted as being due to a weakened hydrophobic effect as well as the participation of an unfavorable partitioning process. Some crossover phenomena were observed in the plots of $\Delta H_{\text{assoc}}^{\circ}$ or $\Delta S_{\text{assoc}}^{\circ}$ versus T (Figure 5b and c) of these nonpolar solutes, indicating that enthalpic and entropic contributions to the binding process depend on the physical state of the Sil-ODA₁₈ phase as well as the molecular nature of the solutes themselves. Collectively, these observations confirm that a highly ordered structure is formed for the Sil-ODA₁₈ sorbent in the crystalline state, with the adsorption of solutes onto the crystalline state and partitioning into the noncrystalline state the dominant retention mechanism.

In the case of conventional *n*-alkylsilicas, solute adsorption has been proposed to be the dominant mechanism of the retention of nonpolar solutes with short *n*-alkyl chain phases, whereas partitioning events have been proposed to occur for longer *n*-alkyl chain phases (i.e., C₈ or longer).¹⁶ Analyte partitioning into the network of bonded *n*-alkyl chains, as encountered in conventional C₁₈ chromatographic sorbents, initially increases with increasing surface coverage until the phase density reaches a value where lateral interactions of neighboring CH₂ groups give rise to *n*-alkyl chain ordering.^{5,6} At higher *n*-alkyl densities, smaller amounts of solutes can partition into the phase because of increasing entropic expulsion of solutes by the grafted *n*-alkyl chains. The chain segment nearest to the support surface is more highly ordered with rapidly increasing disorder toward the chain ends. Hence, solutes will distribute near the chain ends. The retention behavior of the nonpolar solutes with the Sil-ODA₁₈ phase between 291 and 317 K thus appears to be similar to the partitioning effects noted with very high density C₁₈ stationary phases. In contrast, the retention processes of the nonpolar solutes with the Sil-ODA₁₈ sorbent at $T < 291$ K are similar to those manifested by short chain *n*-alkyl phases (i.e., with *n*-alkyl chain lengths less than C₈). The major difference between the Sil-ODA₁₈ phase and conventional *n*-alkyl bonded phases is that the ordering of the Sil-ODA₁₈ phase occurs spontaneously, whereas it depends on the bonding chemistry, ligand density, *n*-alkyl chain length, and choice of mobile-phase conditions for the conventionally bonded *n*-alkylsilica RPC phases.

The shape selectivity of the Sil-ODA₁₈ phase toward the polycyclic aromatic hydrocarbons (PAHs) was observed to change on transition of the phase from the crystalline to the isotropic state, particularly at $T > 293$ K,^{47,48} but the changes were relatively small at $T < 303$ K. For example, the isomeric naphthalene, perylene, and benzo(e)pyrene was observed to

elute in the order of naphthacene > perylene > benzo(e)pyrene at $T = 293$ K, but the elution order gradually changed with the further increase of T , and they eluted in the order of perylene > benzo(e)pyrene > naphthacene at $T > 303$ K.⁴⁸ The small structural changes in the structure of the Sil-ODA₁₈ phase that occurred between $T = 293$ – 303 K were undetectable in the DSC measurement. Furthermore, the T value at which the k' values increased was also observed to be dependent upon the shape and size of PAHs. It was often claimed that the π – π interaction between solutes and carbonyl groups of octadecylacryl groups of Sil-ODA₁₈ side chains contributed to the selectivity enhancement.^{18,49} However, the contribution of π – π interaction to the selectivity enhancement of these analytes could not be separated from other effects in these previous investigations. In the present study, the use of saturated hydrocarbons showed that the differences in T values at which the k' values increased for the PAHs was not solely related to π – π interactions but were dependent on the shape and size of the molecules since these parameters relate to analyte accommodation into the sorbent structure. Moreover, the thermodynamic data obtained for the alkanes and cycloalkanes confirmed that Sil-ODA₁₈ formed an ordered crystalline structure at $T < 291$ K in an 80% methanol/water solvent system, with some structural changes occurring between 291 and 303 K.

A previous preliminary study suggested⁴⁷ that the k' increases with T for nonpolar solutes with the Sil-ODA₁₈ sorbent were related to the contact volumes of the solutes. The present investigations greatly extend these observations on the effect of shape selectivity, indicating that planar and slender solutes are more effectively incorporated into ordered structures of the Sil-ODA₁₈ sorbent than into nonplanar or square-shaped solutes. To our knowledge, there is no *ab initio* theoretical background to accommodate or predict this kind of dependence with comb-shaped ligand sorbent systems (i.e., the relationship between contact volume and retention for anisotropic and isotropic phases). To interpret the findings from the current investigations, we have adapted the molecular theory of chromatography for blocklike solutes (PAHs) in anisotropic and isotropic phases developed by Yan and Martire.^{50–52} When an isotropic stationary phase is replaced by an anisotropic one, enhancement of the shape selectivity experienced by isomeric solutes can arise from the differences in A_{\min} (minimum area) and A_{sur} (total surface area). When nonpolar solutes are enclosed in a box of dimensions $a \times b \times c$ (such that $a < b < c$), then $A_{\min} = ab$ and $A_{\text{sur}} = 2(ab + ac + bc)$. The contact area of a solute with an anisotropic stationary phase, $A_{\text{cont,aniso}} = 2(ac + bc)$, is much smaller than that with an isotropic phase, $A_{\text{cont,iso}} = 2(ab + ac + bc)$. The application of the adsorption and partition retention models to the retention data of the test solutes with the Sil-ODA₁₈ sorbent in the crystalline and the noncrystalline phase states leads to the conclusion that the k' value increases can be accommodated by this adaptation of the Yan–Martire theory. In particular, the retention data shown in Table 1 and Figure 4 indicate that the k' values start to increase in value between 291 and 307 K. As the solute–stationary-phase interaction progresses from a dominant adsorption to a dominant partition mechanism on transition of the phase from the crystalline to noncrystalline state, the contact areas of the solutes gradually increase, and hence they show larger k' values.

Why do the k' values of the nonpolar solutes change in a curvilinear manner as T is varied? As apparent from the DSC results, changes in the phase organization of Sil-ODA₁₈ sorbent between 291 and 303 K were usually small for most mobile-phase combinations. In fact, large changes occurred only at T

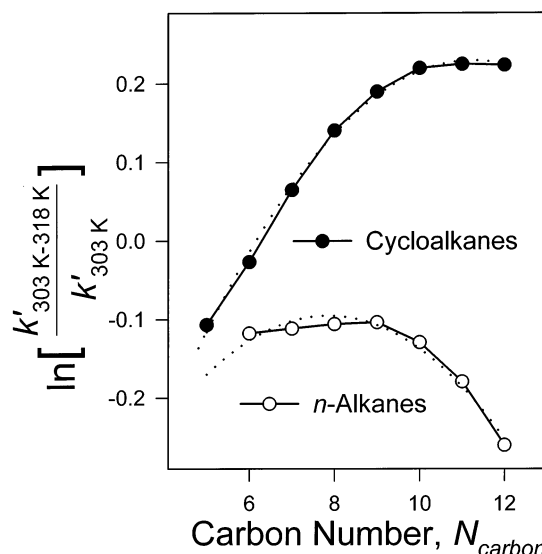


Figure 7. Plots illustrating the relationship between $\ln[(k'_{303 \text{ K} \rightarrow 318 \text{ K}})/k'_{303 \text{ K}}]$ and the carbon number, N_{carbon} , of different cycloalkanes and n -alkanes, showing that the k' -jump effect is related to the shape and size of solute molecules. Regression analyses are shown as the dotted lines for the fit of $\ln[(k'_{303 \text{ K} \rightarrow 318 \text{ K}})/k'_{303 \text{ K}}]$ versus N_{carbon} to a quadratic function, with $r^2 = 0.9965$ and $r^2 = 0.9915$ for the cycloalkanes and n -alkanes, respectively. The experimental conditions were as follows: sorbent, Sil-ODA₁₈; mobile phase, methanol/water (75:25 v/v); and flow rate, 1 mL min⁻¹. Other conditions are given in the Materials and Method section. The solid lines correspond to the first-order fit of the data with the dotted lines corresponding to the 95% confidence limits.

values above 303 K when 80% (v/v) methanol/water was used as the eluent. As discussed above, the extent of partitioning of nonpolar solutes into such mixed-phase systems depends on how much of the phase has transformed to the liquid-crystalline state. When the Sil-ODA₁₈ phase is in this liquid-crystalline state, the nonpolar solutes can be only partially embedded, with some portion of the solutes remaining in contact with the solvent. Therefore, the ratio of the contact area of the solute in association with the stationary phase to the mobile phase determines whether a nonpolar solute will show a k' increase (i.e., the higher the value of this ratio, the greater the possibility for an increase in k' values). This ratio is expected to be higher for small solutes than for larger ones because the penetration is more limited in the latter situation. Hence, the T value will be lower and the k' values will increase in value more for cycloheptane or cyclooctane than for cyclododecane. Similarly, the T dependence at which the k' values for the open-chain n -alkanes increased followed the order of heptane < decane or undecane < dodecane. Because of their flexibility and slenderness, the n -alkanes are expected to be able to penetrate more deeply into the phase than the cycloalkanes and thus show relatively smaller k' increases at lower T values than the cycloalkanes. As solute penetration is limited at T values below 303 K, cycloalkanes will be accommodated more readily than n -alkanes. The contact ratio of solutes embedded in the stationary phase is expected to be higher for cycloalkanes than for n -alkanes. Hence, cycloalkanes show larger k' increases at relatively low T values.

The T -dependent observations shown in Figure 4 and Table 1 can be described in terms of the “ k' -jump” effect, which can be evaluated from the corresponding plots of $\ln[(k'_{303 \text{ K} \rightarrow 318 \text{ K}})/k'_{303 \text{ K}}]$ versus the carbon number of solute homologues such as the n -alkanes and cycloalkanes. These plots confirm that the k' -jump transition is dependent upon the shape and size of the nonpolar solutes (Figure 7). The k' -jump effect increased with

the increasing size of the solutes. Above a certain size, however, the k' -jump value for the cycloalkanes gradually decreased with further increases in the size of solutes. As discussed above, on one hand, partitioning of the nonpolar solute can increase as the phase undergoes a transition from the crystalline to the noncrystalline state, whereas on the other hand, the nonpolar solutes are squeezed out of the phase by the increasing T . In such systems, deep penetration by the nonpolar solute into the phase will be a relatively more favorable process for small solutes than for large solutes, whereas large solutes will tend to be more readily squeezed out at higher T than the small solutes. Because of these penetration and squeezing effects, the relatively large and rigid nonplanar solutes such as *trans*-androsterone ($C_{19}H_{30}O_2$) or cholesterol ($C_{27}H_{46}O$) did not exhibit the characteristic T dependence of liquid-crystalline phases (i.e., a k' increase near the phase transition was not observed (Chowdhury, M. A. J.; Ihara, H.; Hearn, M. T. W. Unpublished data)).

As a general observation, the k' values of the linear n -alkanes were higher on the Sil-ODA₁₈ sorbent at crystalline T values. How can higher k' -jump values then be accommodated for cycloalkanes other than the n -alkanes? As these solutes are retained by the Sil-ODA₁₈ sorbent at the crystalline T values by the adsorption mechanism, solute-stationary-phase contact areas appear to correlate with the planarity of solutes. Open-chain n -alkanes are more planar than cycloalkanes. Hence, n -alkanes will have larger contact areas (e.g., proportional to $2(ab + bc)$) than cycloalkanes when the Sil-ODA₁₈ sorbent is in the crystalline state. However, cycloalkanes will have greater contact areas (e.g., proportional to $2(ab + bc + ca)$) than n -alkanes when the Sil-ODA₁₈ sorbent is in the liquid-crystalline state. Because of the penetration and squeezing effects described above, cyclic molecules are furthermore expected to be accommodated more efficiently by the Sil-ODA₁₈ sorbent in the liquid-crystalline state than n -alkanes. Cycloalkanes will thus have higher k' -jump values. Crossover phenomena between n -alkanes and cycloalkanes in the noncrystalline region also arise from this effect (Figure 4).

As part of their study on the effect of stationary-phase contributions to retention, Vailaya and Horvath¹⁰ considered that changes in the stationary-phase configuration upon varying the mobile-phase composition did not significantly affect the retention behavior. This might be true for some RPC stationary phases such as low-density n -octadecylsilica. However, we believe that this attribute depends on the type of stationary phase. For example, dibenz(*a,h*)anthracene and indeno(*1,2,3-cd*)pyrene could not be separated⁵³ on Vydac 201TP with 90% (v/v) methanol/water, whereas these compounds were resolved with neat methanol. In light of the present investigation, such phenomenological observations can be explained in terms of phase reorganization and the partition mechanism, which predicts that the plots of $\ln k'$ versus mole fraction of organic modifier (i.e., $\ln k'$ versus ψ) for these two compounds will have different slopes. Vailaya and Horvath¹⁰ have further concluded that the extent of solute retention in RPC is governed by the magnitude of the contact area upon binding, which is not affected much by the stationary-phase organization. As apparent from the current investigations, the magnitude of the contact area of a solute in association with the immobilized ligands clearly depends on the stationary-phase organization of the Sil-ODA₁₈ sorbent and reflects the extent of partitioning that the solutes can undergo with the Sil-ODA₁₈ stationary phase in the crystalline and noncrystalline states. This conclusion is consistent with the observation⁵³ that benzo(*ghi*)perylene, diben-

z(*a,h*)-anthracene, and indeno(*1,2,3-cd*)pyrene could not be separated with a monomeric C₁₈ phase but can be resolved with the Sil-ODA₁₈ sorbent at the isotropic T value. An analogous increase in the retention of peptides has been observed in associated investigations with Sil-ODA₁₈ sorbents but not with n -octadecyl-silicas at T values above 328 K (Chowdhury, M. A. J.; Hearn, M. T. W. Unpublished observations, 2001). The retention characteristics of peptides separated on the Sil-ODA₁₈ sorbent in the isotropic state will be reported in a subsequent publication.

Comparison of the Effect of Phase Organization of Bonded n -Alkylsilica and Sil-ODA₁₈ Sorbents on the Retention Behavior of Nonpolar Solutes. Lochmüller and Wilder have proposed⁵⁴ a liquid-droplet model for the bonded n -alkyl chains of conventional RPC sorbents. In this model, the n -alkyl chains collapse and form patches of n -alkyl droplets that permit 3D interactions with the solute molecules. Consistent with this proposal, Wong and co-workers observed⁵⁵ by fluorescence lifetime measurements a collapse of the bonded n -alkyl chains upon their exposure to highly aqueous solvents. Similarly, for n -alkylsilicas, Yarovsky et al.^{56,57} as well as Klatte and Beck^{58,59} have shown by molecular dynamics simulation procedures that the n -alkyl chains are largely collapsed on the silica surface because of self-interaction when a solvent of low elutopicity (high water content) is employed or when the morphology of the stationary phase surface was "rough" on a several-angstroms scale. However, n -alkyl chain extension is expected to occur at high acetonitrile or methanol concentrations. This conclusion is in accord with the observations of Karch et al.⁶⁰ whereby the bonded n -alkyl chains were pictured to adopt a bristlelike structure that extended vertically from the silica surface. Such conclusions are also in agreement with the findings of Sander et al.,⁶¹ who found in their IR measurements that a substantial increase in the order of n -alkyl chains occurred on the addition of an eluent containing a high volume fraction of methanol both at room and lower T values. Moreover, ¹³C MAS NMR spectroscopic studies, compared to data obtained by the conventional solid-state NMR methods, with a C₃₀-silica sorbent have revealed that the intensity of gauche signals increased in the presence of methanol or acetonitrile.^{62,63} This behavior arises because the mobility of the n -alkyl chains increases in such solvents. Alignment of the n -alkyl chains was also dramatically altered in the presence of a strong solvent such as methyl-*tert*-butyl ether, where gauche signals predominated. Zeigler and Maceil have extensively studied the effects of solvent polarity on the mobility of n -alkyl chains by NMR techniques,^{64,65} with the addition of polar solvents increasing the mobility of the n -alkyl chains. In the case of highly loaded phases, n -alkyl chain motion increased with eluents of increasing acetonitrile content, whereas the addition of water induced the C₁₈ chains to clump together in a separate phase, perhaps in a haystack configuration.

With regard to the ligand flexibility and geometrical form of the Sil-ODA_n sorbents, three important factors need to be considered to describe the selectivity enhancement in comparison to the more conventional n -alkyl bonded phases, and these are ordering, rigidity, and mobility of the stationary phases. Zigzag, planar, or all-*trans* conformations are known to predominate for the crystalline state of n -octadecane as revealed by spectral assignments⁶¹ or based on the calculation of Maroncelli et al.^{66,67} The infrared spectra of such crystalline solids notably lack kink (1367 cm^{-1}), double-gauche (1354 cm^{-1}), and end-gauche (1341 cm^{-1}) bands. Significant intensities of the kink, double-gauche, and end-gauche bands were observed in the dry state of the bonded n -alkyl chains. Bonded

phases are folded in the dry state or in the presence of a nonwetting solvent but adopt a more ordered bristle state when the chains are wet (i.e., when they are in solvents of high organic content). However, at least one gauche defect was noted per chain in the bristle state. Compared to the Sil-ODA_n sorbents, the shape-selectivity factors of the *n*-octadecylsilica were poor for water–methanol systems unless the methanol concentration was very high, partly because solvation of the stationary-phase chain was more important.⁶⁸ To assess the effect of this solvation, Cole et al.^{8,11} utilized the shape of van't Hoff plots to evaluate the retention mechanism of various low-molecular-weight solutes with *n*-alkylsilicas in different mobile-phase systems (1-propanol/water, methanol/water, and acetonitrile/water). Selectivity differences between methanol/water and acetonitrile/water systems were attributed to differences in solvation of the stationary phases. Matire and co-workers^{69,70} have also found substantial differences in the thermodynamics of solute retention in methanol/water and acetonitrile/water mobile-phase mixtures. For example, in acetonitrile/water systems, $\Delta H_{\text{assoc}}^{\circ}$ remained constant when the volume fraction of water, θ_w , was ≤ 0.45 but decreased when $\theta_w \geq 0.5$. In contrast, $\Delta S_{\text{assoc}}^{\circ}$ initially increased as the fraction of water increased, reaching a maximum at around $\theta_w = 0.5$, then decreased with increasing θ_w . However, both $\Delta H_{\text{assoc}}^{\circ}$ and $\Delta S_{\text{assoc}}^{\circ}$ decreased steadily with θ_w for the methanol/water system. The differences in the microstructure of these systems is thus a result of hydrogen-bonding effects dominating in the case of alcohol/water mixtures, whereas clustering of acetonitrile molecules around the nonpolar solutes occurs in acetonitrile/water mixtures. It is apparent from these reports that methanol/water or acetonitrile/water provides better selectivity than water or cyclohexane or methyl-*tert*-butyl ether, with the *n*-alkyl chains completely solvated by these latter two solvents. More gauche than trans chain conformations are present in such solvents,^{62,65} with the *n*-alkyl chains more mobile but less ordered in highly solvated environments. However, the *n*-alkyl chains are less ordered in nonwetting solvents. Consistent with this conclusion, Pursch et al.⁷¹ compared two signals in their ¹³C CP/MAS NMR spectroscopic investigations of bonded C₃₀ interphases. One signal belongs to more-rigid chains with trans conformations, and the other one, to more-mobile chains with trans/gauche conformations. More trans conformations were formed as *T* decreased, indicating that the chains had become more rigid and ordered. Sander and co-workers have also noted in their IR spectral assignments of the bonded *n*-alkyl compounds that bend (double-gauche) and kink defects gradually decreased with decreasing *T*.^{61,72}

The dominant adsorption retention mechanism and high selectivity of the Sil-ODA₁₈ phase in the crystalline state strongly indicate that side chains of the immobilized *n*-octadecylacryl polymer are in the trans conformation, resulting in a rigid, extended structure. The conclusion can also be drawn that the mobility of chains of the Sil-ODA₁₈ phase gradually increases from the free end groups of the *n*-octadecylacrylate moieties with increasing *T*. Thus, gauche conformations can be expected to increase gradually with increasing *T* as the phase undergoes a transition from the crystalline to the noncrystalline state. Pesek et al.^{73,74} have studied several liquid-crystalline chromatographic phases (e.g., [4-(allyloxy)-benzoyl]-4-methoxyphenyl covalently bonded to silica) and have found that the mobile phase becomes more and more hostile to ligand ordering with decreasing percentages of the organic solvent. The point of collapse was variable and dependent upon the polarity of the organic modifier. The percentage of organic modifier

required to reach this critical point followed the order methanol > acetonitrile > tetrahydrofuran. Under these conditions, the ligand collapse could lead to an ordering of the organic moiety onto the silica base material because of the closer proximity of the bonded-phase molecules and a concomitant expulsion of the solvent. Consistent with these findings, we have also observed that the Sil-ODA₁₈ phase became more ordered as the polarity of the solvent was increased. Therefore, the distinguishing feature between our novel silica-immobilized, comb-shaped, liquid-crystalline Sil-ODA₁₈ sorbent and conventional *n*-alkyl chain bonded phases is that in the former case the collapse would lead to an ordering of the organic phase on the silica surface whereas a substantially disordered phase occurs for the conventional *n*-alkylsilicas as the polarity of the mobile phase is increased.

As apparent from the above results, distinctive differences exist between the retention behavior of the comb-shaped polymeric Sil-ODA₁₈ and conventional *n*-alkyl chain sorbents. These differences are partly due to the fact that the bonding chemistry used to prepare these two sorbent types is completely different. In the case of the conventionally immobilized *n*-octadecylsilica, the *n*-octadecyl groups are individually bonded onto the silica surface. In the more general case of traditional C_{4–30} *n*-alkylsilicas, the characteristic properties of such phases are related to their chain length and chain density as well as to the type of bonding chemistry (i.e., monomeric or polymeric type). However, with the Sil-ODA₁₈ sorbent the comb-shaped polymer (ODA₁₈) is prepared first and then block immobilized onto the porous silica with *n*-octadecylacryl groups attached to the polymer backbone on alternative carbon atoms (i.e., $-\text{CH}_2-\text{CH}(\text{CO}-\text{O}-\text{C}_{18}\text{H}_{37})-\text{CH}_2-\text{CH}(\text{CO}-\text{O}-\text{C}_{18}\text{H}_{37})-$). This polymer backbone is flexible and can be arranged on the surface of porous silicas such that the octadecylacryl groups are arrayed as a comb-shaped structure, which forms only at the *T* values of crystallinity. As shown above, phase organization of Sil-ODA_n occurs spontaneously. The selectivity of Sil-ODA₁₈ in the crystalline state is comparable to the polymeric *n*-octadecylsilica (C₁₈-type) sorbents and in the isotropic state, to monomeric C₁₈-type sorbents.^{47,53} However, there are significant differences in retention behavior manifested between the Sil-ODA₁₈ and polymeric *n*-alkylsilica phases. With conventional immobilized C_{4–30} silica phases, shape selectivity is significant only when the solutes partition into the phase, whereas both adsorption and partitioning processes can play dominant roles in achieving shape selectivity with the Sil-ODA₁₈ sorbent. Selectivity in the liquid-crystalline region (i.e., at *T* = 303 to 313 K) of the Sil-ODA₁₈ phase can be controlled by very small changes in *T*. Selectivity, particularly shape selectivity, with such sorbent structures arises from the ability of the solutes to intercalate efficiently into the phase network, with planar and slender solutes more efficiently fitting into the ordered structure than nonplanar or square-shaped solutes. Therefore, planar and slender solutes have longer retention times and hence better shape selectivity. When the side chains of the Sil-ODA₁₈ sorbent in the crystalline state are arranged parallel onto the silica surface, the carbonyl groups of octadecylacryl moieties are exposed to the polar solvent. Nonpolar solutes that are rich in π -electron donor groups are expected to be preferably adsorbed onto the ordered, immobilized *n*-alkyl chains of the Sil-ODA₁₈ phase and at the same time have π – π interactions with the carbonyl groups, resulting in selectivity enhancement.⁴⁷ Although it is often assumed that for selectivity enhancement to occur partitioning rather than adsorption of solutes into the stationary phase is more important, it is now apparent from the

present studies that adsorption processes can be equally important for selectivity enhancement.

We have also observed that the T values for the phase transition with the Sil-ODA₁₈ sorbent shift to much lower values with acetonitrile or ethanol than with methanol. The shift in phase-transition T values with the polarity of the solvent indicates that the nonpolar ligand chains become more mobile in less polar environments, as also found for conventional n -alkylsilicas. The distinctive phase transition for the Sil-ODA₁₈ sorbent observed with polar solvents could not be detected with hexane, suggesting that the stationary phase was highly solvated. Consequently, shape selectivity with hexane was not as significant as with, for example, acetonitrile or methanol. It is important to note here that conventional n -alkyl-bonded sorbents are mostly disordered in the highly aqueous environment. In contrast, the Sil-ODA₁₈ sorbent becomes more ordered as the polarity of the solvent is increased, and thus the operational range of the ordered crystalline state is increased. Therefore, this comparison between the Sil-ODA₁₈ and conventional n -alkyl-bonded sorbents reveals that differences in both the modality and contribution of the mobile and stationary phases are important in determining the retention mechanism of these RPC systems.

Conclusions

This study has revealed that stationary-phase organization is an important factor controlling selectivity, particularly shape selectivity, in the RPC system. With the conventional types of immobilized n -alkyl chains (i.e., C_{4–30}) bonded to porous silica, the combined effects of bonding chemistry, surface coverage, and chain length of the stationary phase as well as the polarity of the mobile phase determine the kind of ordered structure and thus the dominant retention mechanism. With the Sil-ODA₁₈ sorbent in the crystalline state, the retention behavior is consistent with adsorption rather than partitioning processes, with the selectivity enhancement with such phases mainly due to the incorporation of solutes into the ordered structure. The unusually high selectivity in the crystalline state of the Sil-ODA₁₈ phase is consistent with the trans conformation of the side chains predominating in these structures. Thermodynamic studies have also confirmed that a highly ordered structure is formed for the Sil-ODA₁₈ phase in the crystalline state, with reorganizational changes occurring between 291 and 303 K that were undetectable by DSC measurements but could be monitored chromatographically. Thus, partitioning of solutes into the polymer network of the Sil-ODA₁₈ phase is possible only when the extension of side chains occurs away from the silica surface at higher T values, with the extent of partitioning depending upon the magnitude of the chain extension. Enthalpy–entropy compensation further demonstrates how the solute–stationary binding process shifts from an adsorptionlike to a partitionlike mechanism as the Sil-ODA₁₈ phase undergoes a transition from a crystalline to a noncrystalline state.

Phase transitions with conventional n -alkylsilica sorbents have been observed for many years but now seem to be quantitatively insignificant when compared to that found for the Sil-ODA_n sorbent. Phase organization of the Sil-ODA₁₈ sorbent is a spontaneous process that does not depend on the phase density. Our novel stationary phase, Sil-ODA₁₈, shows a very specific chain-ordering effect that can be readily fine tuned by T . Therefore, it is now possible to evaluate independently the roles of stationary- and mobile-phase contributions in selectivity enhancement and more precisely determine the effects of T in the RPC separation of both nonpolar and polar solutes such as

peptides and proteins. Examples of such investigations will be reported subsequently.

Acknowledgment. These investigations were supported by the Australian Research Council and Monbusho (Ministry of Education, Science and Culture, Japan).

References and Notes

- (1) Horvath, Cs.; Melander, W.; Molnár, I. *J. Chromatogr.* **1976**, *125*, 129.
- (2) Melander, W. R.; Horvath, Cs. In *High-Performance Liquid Chromatography: Advances and Perspectives*; Horvath, Cs., Ed.; Academic Press: New York, 1980; Vol. 2, p 113.
- (3) Howard, G. S.; Martin, A. J. P. *Biochem. J.* **1950**, *46*, 532.
- (4) Dill, K. A. *J. Phys. Chem.* **1987**, *91*, 1980.
- (5) Dorsey, J. G.; Dill, K. A. *Chem. Rev.* **1989**, *89*, 331.
- (6) Sentell, K. B.; Dorsey, J. G. *Anal. Chem.* **1989**, *61*, 930.
- (7) Vailaya, A.; Horvath, Cs. *J. Chromatogr., A* **1998**, *829*, 1.
- (8) Cole, L. A.; Dorsey, J. G. *Anal. Chem.* **1992**, *64*, 1317.
- (9) Gill, S. J.; Wadso, I. *Proc. Natl. Acad. Sci. U.S.A.* **1976**, *73*, 2955.
- (10) Vailaya, A.; Horvath, Cs. *J. Phys. Chem. B* **1997**, *101*, 5875.
- (11) Cole, L. A.; Dorsey, J. G.; Dill, A. K. *Anal. Chem.* **1992**, *64*, 1324.
- (12) Sander, L. C.; Wise, S. A. *Anal. Chem.* **1989**, *61*, 1749.
- (13) Sander, L. C.; Wise, S. A. *Anal. Chem.* **1984**, *56*, 504.
- (14) Wise, S. A.; Sander, L. C. *J. High Resolut. Chromatogr. Commun.* **1985**, *8*, 248.
- (15) Sander, L. C.; Wise, S. A. *J. High Resolut. Chromatogr. Commun.* **1988**, *11*, 383.
- (16) Tan, L. C.; Carr, P. W. *J. Chromatogr., A* **1997**, *775*, 1.
- (17) DeVido, D. R.; Dorsey, J. G.; Chan, H. S.; Dill, K. A. *J. Phys. Chem. B* **1998**, *102*, 7272.
- (18) Ihara, H.; Sagawa, T.; Nakashima, K.; Mitsuishi, K.; Goto, Y.; Chowdhury, J.; Sakaki, S. *Chem. Lett.* **2000**, 128.
- (19) Hearn, M. T. W.; Zhao, G. *Anal. Chem.* **1999**, *71*, 4874.
- (20) Boysen, R. I.; Jong, A. J. O.; Wilce, J. A.; King, G.; Hearn, M. T. W. *J. Biol. Chem.* **2002**, *277*, 23.
- (21) Witkiewicz, Z. *J. Chromatogr.* **1982**, *251*, 311.
- (22) Pesek, J. J.; Vidensek, M. A.; Miller, M. J. *J. Chromatogr.* **1991**, *556*, 373.
- (23) Jinno, K.; Saito, Y.; Chopra, R. M.; Pesek, J. J.; Fetzer, J. C.; Biggs, W. B. *J. Chromatogr.* **1991**, *557*, 459.
- (24) Terrien, I.; Achard, M. F.; Félix, G.; Hardouin, F. *J. Chromatogr.* **1998**, *810*, 19.
- (25) Hearn, M. T. W. In *Protein Purification: Principles, High Resolution Methods, and Applications*; Janson, J. C., Ryden, L., Eds.; VCH Publishers: New York, 1988; p 239.
- (26) Boysen, R. I.; Wang, Y.; Keah, H. H.; Hearn, M. T. W. *Biophys. Chem.* **1999**, *77*, 79.
- (27) Hearn, M. T. W. In *Theory and Practice of Biochromatography*; Vijayalakshmi, M. A., Ed.; Taylor & Francis Publishers: London, 2001; pp 72–141.
- (28) Boysen, R. I.; Jong, A. J. O.; Hearn, M. T. W. *Biophys. J.* **2002**, *82*, 2279.
- (29) Hearn, M. T. W.; Boysen, R. I.; Wang, Y.; Muraledaram, S. In *Peptide Science*; Shimonishi, Y., Ed.; Kluwer Academic Publishers: Norwell, MA, 1999; pp 240–245.
- (30) Hearn, M. T. W. In *Synthesis of Peptides and Peptidomimetics*; Goodman, M., Felix, A., Moroder, L., Toniolo, C., Eds.; Houben-Weyl-Thieme Publ.: Stuttgart, Germany, 2002. In press.
- (31) Vailaya, A.; Horvath, Cs. *J. Phys. Chem.* **1996**, *100*, 2447.
- (32) Privalov, P. L.; Gill, S. J. *Adv. Protein Chem.* **1988**, *39*, 191.
- (33) Murphy, K. P.; Privalov, P. L.; Gill, S. J. *Science (Washington, D.C.)* **1990**, *247*, 903.
- (34) Vailaya, A.; Horvath, Cs. *Ind. Eng. Chem. Res.* **1996**, *35*, 2964.
- (35) Haidacher, D.; Vailaya, A.; Horvath, Cs. *Proc. Natl. Acad. Sci. U.S.A.* **1996**, *93*, 2290.
- (36) Tanford, C. *The Hydrophobic Effect: Formation of Micelles and Biological Membranes*, 2nd ed.; Wiley: New York, 1980.
- (37) Dill, K. A. *Science (Washington, D.C.)* **1990**, *250*, 297.
- (38) Dill, K. A. *Biochemistry* **1990**, *29*, 7133.
- (39) Southall, N. T.; Dill, K. A. *J. Phys. Chem. B* **2000**, *104*, 1326.
- (40) Murphy, K. P.; Privalov, P. L.; Gill, S. J. *Science (Washington, D.C.)* **1990**, *247*, 559.
- (41) Marqusee, J. A.; Dill, K. A. *J. Chem. Phys.* **1986**, *85*, 434.
- (42) Spolar, R. S.; Ha, J. H.; Record, M. T., Jr. *Proc. Natl. Acad. Sci. U.S.A.* **1989**, *86*, 8382.
- (43) Murphy, K. P.; Gill, S. J. *J. Mol. Biol.* **1991**, *222*, 699.
- (44) Seelig, J.; Ganz, P. *Biochemistry* **1991**, *30*, 9354.

- (45) Wimley, W. C.; White, S. H. *Biochemistry* **1993**, 32, 6307.
- (46) Ross, P. D.; Rekharsky, M. V. *Biophys. J.* **1996**, 71, 2144.
- (47) Chowdhury, M. A. J.; Ihara, H.; Sagawa, T.; Hirayama, C. *J. Chromatogr., A* **2000**, 877, 71.
- (48) Chowdhury, M. A. J.; Ihara, H.; Sagawa, T.; Hirayama, C. *J. Liq. Chromatogr. Relat. Technol.* **2000**, 23, 2289.
- (49) Ihara, H.; Sagawa, T.; Goto, Y.; Nagaoka, S. *Polymer* **1999**, 40, 2555.
- (50) Yan, C.; Martire, D. E. *Anal. Chem.* **1992**, 64, 1246.
- (51) Yan, C.; Martire, D. E. *J. Phys. Chem.* **1992**, 96, 3489.
- (52) Yan, C.; Martire, D. E. *J. Phys. Chem.* **1992**, 96, 3505.
- (53) Chowdhury, M. A. J.; Ihara, H.; Sagawa, T.; Hirayama, C. *Chromatographia* **2000**, 52, 45.
- (54) Lochmüller, C. H.; Wilder, D. R. *J. Chromatogr. Sci.* **1979**, 17, 574.
- (55) Wong, A. L.; Hunnicutt, M. L.; Harris, J. M. *Anal. Chem.* **1991**, 63, 1076.
- (56) Yarovsky, I.; Aguilar, M. I.; Hearn, M. T. W. *J. Chromatogr.* **1994**, 660, 75.
- (57) Yarovsky, I.; Aguilar, M. I.; Hearn, M. T. W. *Anal. Chem.* **1995**, 67, 2145.
- (58) Klatte, S. J.; Beck, T. L. *J. Phys. Chem.* **1995**, 99, 16024.
- (59) Klatte, S. J.; Beck, T. L. *J. Phys. Chem.* **1996**, 100, 5931.
- (60) Karch, K.; Sebastian, I.; Halasz, I. *J. Chromatogr.* **1976**, 122, 3.
- (61) Sander, L. C.; Callis, J. B.; Field, L. R. *Anal. Chem.* **1983**, 55, 1068.
- (62) Strohschein, S.; Pursch, M.; Lubda, D.; Albert, K. *Anal. Chem.* **1998**, 70, 13.
- (63) Pursch, M.; Sander, L. C.; Albert, K. *Anal. Chem.* **1999**, 71, 733A.
- (64) Zeigler, R. C.; Maciel, G. E. *J. Phys. Chem.* **1991**, 95, 7345.
- (65) Zeigler, R. C.; Maciel, G. E. *J. Am. Chem. Soc.* **1991**, 113, 6349.
- (66) Maroncelli, M.; Qi, S. P.; Strauss, H. L.; Snyder, R. G. *J. Am. Chem. Soc.* **1982**, 104, 6237.
- (67) Maroncelli, M.; Qi, S. P.; Snyder, R. G.; Strauss, H. L. *Science (Washington, D.C.)* **1981**, 214, 188.
- (68) Sander, L. C.; Wise, S. A. In *Retention and Selectivity in Liquid Chromatography*; Smith, R. M., Ed.; Journal of Chromatography Library; Elsevier Science: New York, 1995; Vol. 57, p 337.
- (69) Alvarez-Zepeda, A.; Barman, B. N.; Martire, D. E. *Anal. Chem.* **1992**, 64, 1978.
- (70) Stalcup, A. M.; Martire, D. E.; Wise, S. A. *J. Chromatogr.* **1988**, 442, 1.
- (71) Pursch, M.; Strohschein, S.; Händel, H.; Albert, K. *Anal. Chem.* **1996**, 68, 386.
- (72) Sander, L. C.; Pursch, M.; Wise, S. A. *Anal. Chem.* **1999**, 71, 4821.
- (73) Pesek, J. J.; Siouffi, A. M. *Anal. Chem.* **1989**, 61, 1928.
- (74) Pesek, J. J.; Lu, Y.; Siouffi, A. M.; Grandperrin, F. *Chromatographia* **1991**, 31, 14.